Science Progress (2011), 94(1), 16–96
doi: 10.3184/003685011X12982218769939

Electron spin resonance. Part one: A diagnostic method in the biomedical sciences

CHRISTOPHER J. RHODES

ABSTRACT

A review is presented of some of the ways in which electron spin resonance (ESR) spectroscopy may be useful to investigate systems of relevance to the biomedical sciences. Specifically considered are: spin-trapping in biological media; the determination of antioxidant efficiencies; lipid-peroxidation; the use of nitroxides as probes of metabolic activity in cells and as structural probes of cell-membranes; ESR coupled with materials for radiation-dosimetry; food- and drug-irradiation; studies of enzyme systems and of cyclodextrins; diagnosis of cancer and rheumatoid arthritis; measurement of oxidative stress in synovial tissue in preparation for joint replacement; determination of oxidative species during kidney dialysis; measurement of biological oxygen concentrations (oximetry); trapping in living cells of the endothelium-derived relaxing factor nitric oxide (NO); measurement of hydrogen peroxide; determination of drugs of abuse (opiates); ESR measurements of whole blood and as a means to determine the age of bloodstains for forensic analysis are surveyed, and also a determination of the aqueous volume of human sperm cells is described, among other topics.

Keywords: *electron spin resonance, antioxidant efficiencies, lipid-peroxidation, structural probe of cell-membranes, diagnosis of cancer and rheumatoid arthritis, biological fluids*

Professor Chris Rhodes has a visiting position at the University of Reading and is Director of Fresh-lands Environmental Actions. He has catholic scientific interests (www.fresh-lands.com) which cover radiation chemistry, catalysis, zeolites, radioisotopes, free radicals and electron spin resonance spectroscopy, which more recently have developed into aspects of environmental decontamination and the production of sustainable fuels. Chris has given numerous radio and televised interviews concerning environmental issues, both in Europe and in the United States – including on BBC Radio 4's Material World. Latest invitations include a series of international Cafe' Scientifique lectures regarding the impending depletion of world oil and the need to develop oil-independent, sustainable societies. He has published more than 200 peer-reviewed scientific articles and five books. He is also a published novelist, journalist and poet. His novel ''University Shambles'' has just been released as an eBook and has been nominated for Brit Writers' Awards 2011: Published Writer of the Year.
E-mail: cjrhodes@fresh-lands.com

1. Introduction

Electron spin resonance (ESR) – also known as electron paramagnetic resonance (EPR) – is often viewed as the Cinderella sister of nuclear magnetic resonance (NMR). This is partly because both the application and availability of NMR spectrometers are more apparent, and that not uncommonly ESR receives only passing mention in university courses, unless there is a specialist in the subject on the staff. In principle, NMR spectra may be recorded from dozens of different nuclei, whereas obtaining an ESR spectrum requires some of the sample molecules to contain one or more unpaired electrons, which might appear to be an oddity. Notwithstanding, here lies the beauty of ESR, since the method is completely specific for unpaired electrons, which are frequently formed in materials that have encountered one or more of a range of important energetic conditions for which a signature is supplied in the form of the consequent ESR spectrum. The unpaired electron bearing sites are usually termed ''damage centres'', ''defects'' or ''trapped electrons'' by physicists, geologists, archeologists and environmental scientists, but are normally referred to by chemists and biologists as ''free radicals'', whose detailed molecular structures may be revealed from the spectral parameters of hyperfine splitting, where it is observed, and of g-factor.

Paramagnetic transition-metal cations, *e.g.* Fe^{3+}, Mn^{2+}, Cu^{2+}, are commonly detected in environmental samples and in biological

tissues using ESR. Paramagnetic materials, including metal cations and synthesised complexes or stable organic radicals (usually nitroxides), may be deliberately added to samples as probes of local molecular environments such as cell-membranes, and to determine their dynamic properties. Along with other stable ''organic'' radicals (*e.g.* carbon chars and lithium phthalocyanines), nitroxides may be used to measure oxygen tensions in whole tissues and in simpler cellular systems. Metabolic activities in such biological media may also be determined from the reduction kinetics of nitroxides. When it is desired to investigate various reacting systems for the intermediacy of free radicals, ''spin-traps'' are often added. These are frequently of a structural type designed to ''trap'' reactive radicals by addition to them, so forming nitroxides *in situ*, which rise to detectable concentrations in consequence of their relative stability. Clearly, there are many and varied important applications for ESR, and most importantly so in areas of the biological and environmental sciences.

2. The ESR Experiment[1]

2.1 Background and scope

ESR (electron spin resonance) is also referred to as EPR (electron paramagnetic resonance), and as already noted is a method of magnetic resonance spectroscopy which measures unpaired electrons, specifically. It is, therefore, implicitly more restricted in its applications than is NMR (nuclear magnetic resonance)[1], which in its various adaptations, measures a comprehensive range of magnetic nuclei; but therein lies the advantage and subtlety of ESR. Unpaired electrons are created in a broad variety of samples which have often encountered fairly extreme conditions; *e.g.* high-energy (ionising) radiation (X-rays, γ-rays), energetic particles (electrons, protons, α-particles UV light, high temperatures, combustion processes, reactive chemical reagents, mechanical stress, explosions. As we shall see, under both these and other sets of conditions, structural dislocations may be introduced in the form of organic and inorganic free radicals, which host unpaired electrons, and their ESR signal may provide a marker of the kind of process which has created them. The great power of ESR is its ability to identify the chemical nature of free radical species, and from the intensity and line-widths of the signal the number of radicals that have been formed and various features of the local molecular environment in the sample may further be deduced.

Free radicals, moreover, play a central role in Nature, particularly in living systems, and consequently, current activity in researching into these species is enormous. Mainly, this is because it is widely held, and this in part through the agency of ESR measurements, that radicals provide both the cause and mediation of many diseases, and indeed of the ageing process itself. The generally reactive character of radicals and unpaired-electron species overall (including metal ions, which can participate in redox processes) further underpins much of chemistry (it is, of course, ''chemistry'' which is implicit to all the above), and it is largely on the findings from simpler chemical systems that much of current biochemical thinking is based, and this underlying free radical chemistry impacts further on a variety of environmental aspects – especially in the role of pollutants in atmospheric phenomena, such as ozone-loss, global warming and acid-rain production. Furthermore, since the atmosphere is in direct contact and exchange with the surface of the Earth – with the soil, the plants which grow within and upon it (biosphere), the rocks and mountains (lithosphere), and the rivers, seas and oceans (hydrosphere) – the chemistry of the atmosphere takes on a wider role. [This will be discussed in more detail in a separate review.] Remarkably, ESR can provide insight into many of these phenomena too, both through its use in the investigation of model systems, and more directly as an analytical technique.

2.2 The basis of the experiment itself

The basic EPR experiment rests upon entirely similar principles to those which underpin NMR spectroscopy, but the method is specific for detecting molecules with unpaired electrons – namely free radicals and certain metal (usually transition metal) complexes. EPR spectra are characterised by (i) g-factors (g-values) and (ii) hyperfine coupling constants, which are in analogy with (i) chemical shifts and (ii) spin – spin couplings in NMR. It may be helpful to first consider the, *e.g.* ^{1}H, NMR experiment, since a proton (^{1}H), like an electron, has a spin of *one half* ($\frac{1}{2}$); the nuclear spin being designated as $I = \frac{1}{2}$, with quantum numbers (labels) $m_I = +\frac{1}{2}, -\frac{1}{2}$, while the electron spin is designated as $s = \frac{1}{2}$, with quantum numbers $m_s = +\frac{1}{2}$ or $-\frac{1}{2}$. We now compare and contrast these two distinct methods.

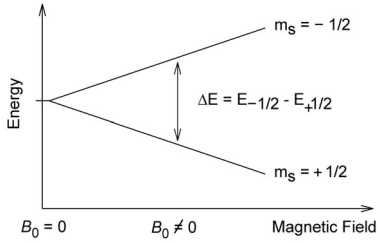

Figure 1 *Splitting of nuclear spin energy levels by an external magnetic field (B) in an ^1H NMR experiment. Credit J. Bancroft Brown. http://upload.wikimedia.org/wikipedia/en/6/67/NMR_splitting.gif*

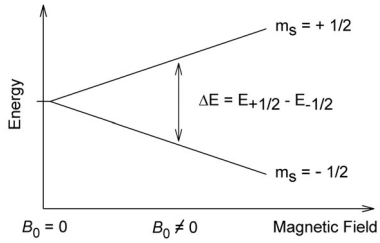

Figure 2 *Splitting of electron spin energy levels by an external magnetic field (B) in an ESR experiment. Credit Nicolas Guérin. http://upload.wikimedia.org/wikipedia/commons/a/a9/EPR_splitting.jpg*

2.2.1 ^1H NMR[1]

In the absence of an external magnetic field, protons with spin $+\frac{1}{2}$ or $-\frac{1}{2}$ have the same energy; however, as the field is applied, those $+\frac{1}{2}$ are lowered, and those $-\frac{1}{2}$ are raised in energy, relative to the zero field situation (Figure 1). There is, therefore, an energy level *splitting* introduced between the $m_I = +\frac{1}{2}$ and $m_I = -\frac{1}{2}$ states, by the external magnetic field. [One can imagine the spinning proton (hydrogen nucleus) behaving as a tiny magnet, which senses the influence of the far stronger external magnetic field]. The energy level splitting is described by [Eqn (1)]:

$$\Delta E = g_N \mu_N B(1 - \sigma) \tag{1}$$

g_N and μ_N are constants (respectively the ''nuclear g-factor'' and the ''nuclear magneton'') which define the intrinsic magnetic field strength of a given spinning nucleus, while σ, the ''chemical shift'', determines the strength of the magnetic interaction between the external magnetic field (B) and the nucleus (proton). σ-Values are not normally determined directly, but ''chemical shifts'' are generally labelled δ, and quoted relative to some standard (*e.g.* TMS, Me_4Si) in parts-per-million of the external magnetic field strength. Either way, σ or δ, the chemical shift represents the local electronic environment of the proton, which resonates diagnostically at different magnetic field values, according to the kind of chemical functional group that it occupies.

2.2.2 ESR[1]

A single unpaired electron can adopt either the spin $m_s = +\frac{1}{2}$ or $-\frac{1}{2}$ state. In the absence of an external magnetic field, both states have the same energy. Statistically, therefore, when a large number of unpaired electron species (free radicals or metal ions, *e.g.* Mn^{2+}, Fe^{3+}, Cu^{2+}) are present together in a given sample, there is an equal number of each state present (*i.e.* 50 : 50; $-\frac{1}{2}:+\frac{1}{2}$). When an external magnetic field is applied (Figure 2) this is no longer the case, and an excess population of $m_s = -\frac{1}{2}$ appears, since not only is the energy of this state lowered, but that of the $m_s = +\frac{1}{2}$ state is increased by their interaction with the applied field. [As in the NMR case of the proton, above, one can imagine the spinning electron behaving as a tiny magnet, which feels, therefore, the influence of the far stronger external field]. This may be represented by [Eqn (2)], where E_o is the energy of both $m_s = +\frac{1}{2}$ or $-\frac{1}{2}$ states before the magnetic field is applied (μ_B is the Bohr magneton).

$$Em_s = E_o + g\mu_B B m_s \tag{2}$$

The energy difference (ΔE) between the states $m_s = +\frac{1}{2}$ or $-\frac{1}{2}$ is, therefore, given by [Eqn (3)], and is seen to increase in direct proportion to the strength of the external magnetic field (B). In ESR, it is the g-factor [given in Eqn (3)] that is quoted directly as the variable parameter which renders a different ΔE for each type of radical, rather than quoting a chemical shift as is done in NMR. As in a nucleus in NMR, of course, the unpaired electron will resonate at a different magnetic field strength according to the kind of molecular species (radical or metal ion) that it occupies.

$$\Delta E = g\mu_B B \tag{3}$$

This situation for ESR may be represented as in Figure 2, in which the external magnetic field has caused an energy level splitting between the levels associated with the $m_s = +\frac{1}{2}$ or $-\frac{1}{2}$ states. While helpful comparisons may be drawn between ESR and NMR, there are some essential differences, too. For example, as already described, (and as is clear from Figures 1 and 2), in ESR it is the $-\frac{1}{2}$ level whose energy falls, while that of the $+\frac{1}{2}$ state increases: this reversal in behaviour with respect to the ^1H NMR experiment is due to the *negative* electron magnetic moment (Bohr Magneton), μ_B, which partly determines the extent of the splitting, according to Eqn (3), and so the energy levels are simply *reversed*. μ_B is also very much larger than μ_N, and so the energy level splitting is accordingly increased, and to the extent that microwave radiation is

required to ''match'' the energy level separation, rather than the radiofrequencies which are used in NMR. [For an external field (B) of 0.3 T, radiation of frequency *ca* 9.4 *G*Hz is required to match the ESR energy level separation, but only *ca* 13 *M*Hz would be needed for ^{1}H NMR]. Due to the energy difference (ΔE) between them [Eqn (3)], the collection of unpaired electron spins is distributed between the two states $m_s = +\frac{1}{2}$ or $-\frac{1}{2}$, whose relative populations are given by a Boltzmann distribution [Eqn (4)],

$$n(+\tfrac{1}{2})/n(-\tfrac{1}{2}) = \exp(-\Delta E/RT) \qquad (4)$$

If the sample is exposed to a source of microwave radiation, whose energy matches ΔE, a ''resonance'' occurs with the unpaired electrons, in which those with spin $m_s = -\frac{1}{2}$ can absorb energy and are promoted (excited) to the higher energy $m_s = +\frac{1}{2}$ state (Figure 2); while their spin $m_s = +\frac{1}{2}$ counterparts can emit an equal amount of energy, and fall back to the $m_s = -\frac{1}{2}$ level. Since the microwave field is equally capable of stimulating a spin-transition in either direction, if the populations of the two states were equal, there would be no overall effect of the ''resonance'', since the absorption and emission of energy would simply cancel one another. But, because there is an overall excess of the $m_s = -\frac{1}{2}$ population, as noted earlier, there is a net absorption of energy. [This holds so long as the detailed mechanisms which allow the return of the unpaired electrons in the excited state $m_s = +\frac{1}{2}$ to the ground state $m_s = -\frac{1}{2}$ are relatively efficient, so the process is *fast*. If the mechanisms are rather inefficient, or the microwave power level is very high, the two states rapidly become equally populated, and the signal intensity falls to zero. This condition is called ''Saturation''].

2.3 ESR instrumentation

2.3.1 Multi-frequency ESR[2]

A specimen ESR spectrometer is shown in Figure 3. The microwave radiation used in ESR is most commonly of frequency *ca* 9–10 GHz [*i.e.* $(9-10)\times10^{9}$ s^{-1}]–the so-named ''X-band''–but other frequency ranges are sometimes used. When a different choice of microwave frequency is made, a different strength of the external magnetic field is required to achieve the resonance condition. This follows from Eqn (4), according to which it is also clear that as the frequency decreases, a smaller excess spin-population occurs in the ground state $n(-\frac{1}{2})$. Since the innate

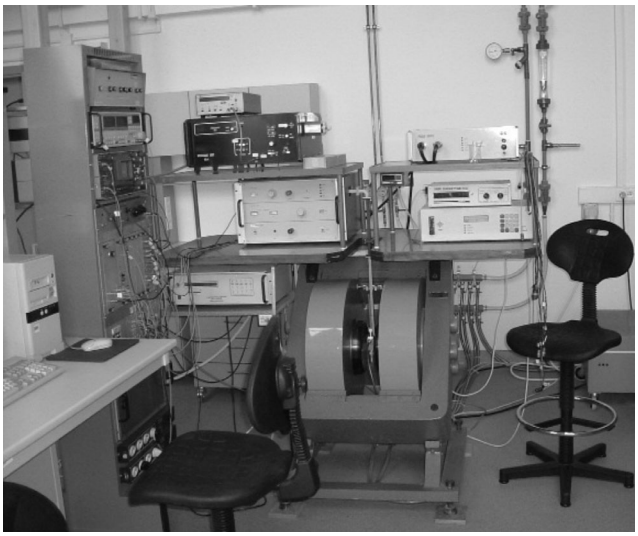

Figure 3 *Specimen ESR spectrometer. Credit Nicolas Guérin. http://upload.wikimedia.org/wikipedia/commons/1/19/EPR_spectometer.JPG*

sensitivity of ESR depends on the ratio $n(+\frac{1}{2})/n(-\frac{1}{2})$, which relates to the Boltzmann factor, it is clear that measurements made at lower microwave frequencies will afford an intrinsically weaker signal. There are, however, very good reasons for undertaking so called ''multi-frequency'' experiments. For example, in the study of large biological or aqueous samples (including isolated organs, such as the liver, and whole, small animals), a frequency of *ca* 1.5 GHz (''L-band'')–or even lower frequencies–is often beneficial. This is because the absorption of microwave radiation by water becomes increasingly attenuated on reduction of its frequency. It is also important to be aware of the ''dimensions'' attendant to the experiment: namely the size of the resonant cavity. At X-band, the frequency (ν) is *ca* 9.5×10^9 s^{-1}, which corresponds to a wavelength (λ) of 3.2 cm. In order to set-up a resonant (standing) wave, the cavity must also be of this dimension. At L-band, since $\nu = 1.5 \times 10^9$ s^{-1}, the size of the cavity is now 20 cm (8 inches!), and so a far larger sample might be accommodated. Allowing, overall, for the loss of sensitivity caused by the reduced Boltzmann factor at the lower frequency, and the compensation for this that is possible with a much larger sample volume, a working rule is that an L-band experiment is of around a factor of ten lower in sensitivity than one at X-band. Similar reasoning applies to measurements made at higher frequencies. For example,

Table 1 *Frequency ranges, wavelengths and resonant magnetic fields for different microwave bands*

Band	ν(GHz)	λ(cm)	B(G)
L	1.5	20	500
S	3	10	1,000
X	9.5	3.2	3,400
K	24	1.3	8,500
Q	35	0.8	12,100
W	94	0.3	33,500
D	140	0.2	49,000

at W-band, $\nu = 9.4 \times 10^{10}\ s^{-1}$. In this case, $\lambda = 0.32$ cm (*ca* 3 mm), and the sample is usually contained in a tube of overall diameter *ca* 1 mm, with an internal diameter of *ca* 0.6 mm. While it is true that the experiment is ideal for (highly expensive) biological materials, available only in small quantities, and that the greatly increased Boltzmann factor will largely offset the loss of sensitivity from such a small sample, the actual signal intensity is limited by problems of magnetic field inhomogeneity and component construction. The commonly encountered microwave frequencies, their wavelength equivalents and attendant magnetic fields required for resonance, are all listed in Table 1, although we note that ESR experiments have been done at frequencies up to *ca* 500 GHz.

Multi-frequency methods are generally resorted to in an effort to improve the resolution of a given ESR spectrum. In the solid-state, it is sometimes unclear whether an apparent splitting arises from different g-components, or is due to hyperfine coupling. By increasing the frequency, the separation of g-components is increased, but a hyperfine splitting will be unaffected. In other cases, g-components may not be fully resolved, but become so at a higher frequency.

A range of frequencies from Table 1 has been applied to a frozen sample containing a nitroxide, in which the radical molecules tumble only slowly, the results of which are evident in Figure 4. At X-band (9 GHz), the triplet splitting from ^{14}N in the ''parallel'' direction in seen, and the intensities of the low-field and high-field lines are about equal, because the g-anisotropy presents only a very small splitting at this low frequency. Nor is there any resolved ''perpendicular'' ^{14}N splitting on the central feature. However, as the frequency is increased, there is a progressive separation of the g-components, until, at D-band (140 GHz), they are fully resolved.

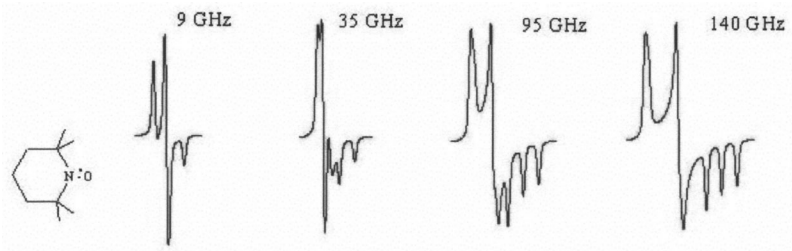

Figure 4 *ESR spectra of the nitroxide shown in a solid frozen medium and tumbling slowly, as a function of the frequencies shown. Credit Astrochemist. http://upload.wikimedia.org/wikipedia/en/8/8e/EPR_multifrequency_spectra.jpg*

The parallel splitting is now clear on the highest-field g-feature, and incipient (perpendicular) splitting is now evident on both the other g-features if they are inspected closely. At the lower frequencies, overlap between these components diffuses their detail into the linewidths. In other experiments, this time for rapidly-tumbling nitroxides, used to probe a distribution of aqueous and lipid phases present simultaneously in a given sample, *e.g.* liposomes the two environments are readily identified at W-band, since a smaller isotropic g-factor is conferred to a nitroxide in the aqueous medium, while (as noted in Section 4), the isotropic ^{14}N coupling is simultaneously increased. Thus two separate spectra are visible from the two environments. At X-band, there is often considerable overlap between the signals from the two components.

2.3.2 In-vivo *ESR*[3]

By means of low-frequency ESR, *e.g.* at L-band or lower, it is possible to examine biological samples including whole animals, or, say, the arm of a human volunteer (or the leg, if they were sufficiently thin). For the most part, stable nitroxides have been introduced into animal subjects (rats and mice) which can be detected *in vivo* (Figure 5). Human subjects have mostly been studied from the point of view of oximetry (Section 6), *i.e.* to measure the oxygen concentration in tissue using the paramagnetic line-broadening that is caused by Heisenberg spin-exchange between the unpaired electrons in stable free-radicals present in the tissue *e.g.* skin, and those in dioxygen molecules, which have a triplet electronic state (two unpaired electrons). In Figure 6 is shown an experimental arranagement, still under development, for performing oximetry on whole human subjects with a 50 cm cavity.

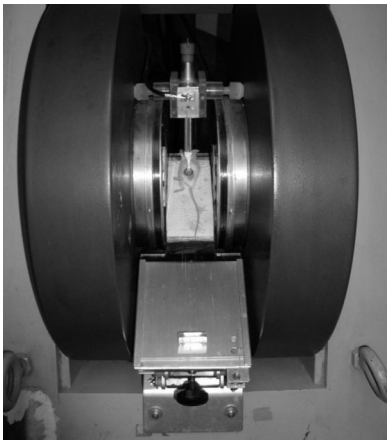

Figure 5 *Experimental arrangement for performing oximetry on whole small animals at the laboratory of biophysics–EPR centre Ljubljana. Reproduced with permission. http://www.ijs.si/ijs/dept/epr/dosimetry.html*

Figure 6 *Experimental arrangement for measuring oxygen concentrations in human subjects at the Dartmouth Medical School with a 50 cm sample cavity. Note vast difference in size from the set-up in Figure 5. Reproduced with permission. http://www.dartmouth.edu/~eprctr/research/tooth_dosimetry.shtml*

In vivo ESR has also been used to determine high radiation-dose exposures, from the signals engendered in tooth enamel[4]. As a result of terrorism, accident or war, there is the potential risk that populations might be exposed to doses of ionising radiation sufficient to cause direct clinical effects within days or weeks. There is a critical need to determine the magnitude of the exposure to individuals so that those with significant risk can have appropriate procedures initiated immediately, while those without a significant probability of acute effects can be reassured and removed from the need for further consideration by the medical/emergency team (*i.e.* to establish a triage system). It is extremely unlikely that adequate dosemeters will be worn by the potential victims, and nor is it probable that prompt and accurate dose reconstruction will be possible on an individual basis. *In vivo* EPR measurements of radiation-induced changes in the enamel of teeth provide perhaps the only method able to differentiate among doses sufficiently to classify individuals into categories for treatment accurately enough to facilitate decisions on medical treatment. In its current state, the *in vivo* EPR dosemeter can provide estimates of absorbed dose with an error of $\pm$ 0.5 Gy in the range 1–10 Gy. The lower limit and the precision are expected to improve, with

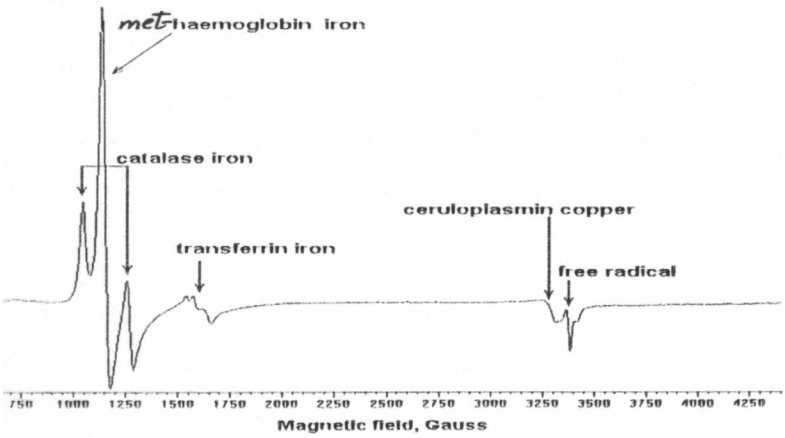

Figure 7 *EPR spectra of blood following measured at 10 K illustrating the following spectral features: high-spin ferric haem iron in catalase, high-spin ferric haem iron in methaemoglobin, high-spin ferric non-haem iron in transferrin, cupric copper in ceruloplasmin, globin free radical.*

better resonators and algorithms for acquiring and calculating the dose. Even in its current state of development, the method is nonetheless already good enough to decide among individuals with regard to acute effects from exposure to ionising radiation for most applications related to terrorism, accidents or nuclear warfare.

3. Biological fluids – blood and plasma

Biological fluids may be examined directly using ESR, *e.g.* blood and plasma, since intrinsic metal-complexes are readily identifiable[5], along with a free-radical component (Figure 7). Thus detectable are high-spin ferric iron from catalase, methaemoglobin and transferrin, and Cu^{2+} in ceruloplasmin along with a globin free radical. Catalase is the essential enzyme responsible for the decomposition of hydrogen peroxide produced by the dismutation of superoxide anions in cells which arises from the fact that animals breathe molecular oxygen. Catalase has one of the highest turnover numbers of all enzymes; one molecule of catalase can convert 40 million molecules of hydrogen peroxide to water and oxygen each second. Without catalase, living cells would be subject to severe attack from $^{\bullet}OH$ radicals (oxidative stress) arising from the reaction between H_2O_2 and free (unbound) iron or other metal cations. Methaemoglobin is the ferric form of haemoglobin, and which

cannot bind oxygen. Transferrin is a blood plasma protein for iron-delivery. Around 70% of the copper present in humans is bound in the form of ceruloplasmin, a protein that is also involved with iron metabolism. The globin radical is formed from methaemoglobin by reaction with peroxides including H_2O_2.

3.1 Determination of the age of bloodstains[6]

The method has also been applied for the forensic analysis of bloodstains to determine their age and hence length of time since bleeding occurred.

Measured at 77 K, human bloodstains give four striking EPR signals in the $g = 6.2$ (g6), 4.3 (g4), 2.27 (H) and 2.005 (R) regions due to ferric high-spin, ferric non-heme, ferric low-spin and free radical species, respectively. From a double logarithmic plot of the EPR intensity ratio of H/g4 versus time since bleeding occurred, a linear correlation was obtained over a period of 432 days to an error of 25% under controlled conditions. However, environmental factors such as differences of absorbent, light exposure and fluctuations of storage temperature were found to influence the results. Haemoglobins in dried bloodstains are decomposed by a combination of chemical and physico-chemical reactions, while enzymatic decomposition processes can be excluded since they require an aqueous environment. The ESR method for estimating the age of human bloodstains has the advantage that it is non-destructive and that a mere 10 mg of dried blood is sufficient to estimate the age of a bloodstain. That said, it is necessary to prepare standard bloodstained materials appropriate to each sample, and a calibration curve under the same conditions, otherwise considerable discrepancies may arise leading to false forensic conclusions as to when bleeding actually took place.

4. Spin-trapping

ESR is extremely useful in revealing very precise details of the structure of free radicals, and identifying them in the first place; but mainly from systems whose chemistry has been pre-empted to produce radicals in relatively high concentrations, or to produce radicals which are stable, and hence long-lived. In the case of radicals which are reaction intermediates, their concentration is typically low (as is true of all reactive intermediates), in reference to the sensitivity of ESR, since they are reactive and are destroyed

by rapid termination processes[7]. The threshold of X-band ESR detection is at a concentration of free-radicals of *ca* 10^{-7} M;[8] however, very few free radicals, especially those involved in biological systems, have sufficiently long lifetimes to maintain a steady-state concentration above this threshold limit. We are therefore confronted by a seemingly insurmountable problem, that ESR is unable to detect radicals in real reacting systems which we desire to explore for the intermediacy of these reactive intermediates. Almost all reacting systems, especially those inherent to biology, suffer from this drawback. The direct observation of free radicals in complex biological systems is nearly always bedevilled by their high reactivity, and hence short lifetimes and low concentrations. Moreover, those radicals most sought in biological systems, those of the so-called reactive oxygen intermediate (ROI), or reactive oxygen species (ROS) class, namely $HO^{\bullet}$ (hydroxyl), $O_2^{\bullet -}$ (superoxide), $HO_2^{\bullet}$ (hydroperoxyl), $RO_2^{\bullet}$ (peroxyl, *generally*), $RS^{\bullet}$ (thiyl), $NO^{\bullet}$ (nitric oxide), all have highly anisotropic g-factors, leading to broad lines in their ESR spectra which mostly would not be detected.

Fortunately, chemical interventions can be exploited to intercept (trap) short-lived radicals, so that their ''adducts'' may accumulate to concentrations sufficiently high for ESR detection. There are, in free-radical chemistry, various interventions for intercepting radicals, which are in the general context termed ''radical scavenging'' or ''radical trapping'', but are focused in the ESR context under the banner of ''spin-trapping'' since ideally, there is no loss of unpaired-electron species (radicals; with unpaired-electron ''spin''), and so the total number of ''spins'' detected by ESR is that of the radicals formed initially in the system under investigation. Reality provides, as ever, rather less than the perceived ideal, and particular compensations are required, especially in studies of living cells; such background details, pros and cons, merits and troubles all inherent to spin-trapping are now considered.

4.1 Spin-trapping chemistry

In most practical situations, the radical ''trap'' (''spin-trap'') is a *nitrone* or a *nitroso* compound. These possess diamagnetic molecules (without unpaired electrons, ''spins''), which are able to ''trap'' a reactive short-lived radical in an addition reaction, Scheme 1, so that relatively long-lived $R_2N-O^{\bullet}$ radicals are produced (e.g. Figure 8), thus allowing an accumulation above the limits of ESR detection. $R_2N-O^{\bullet}$ radicals are variously

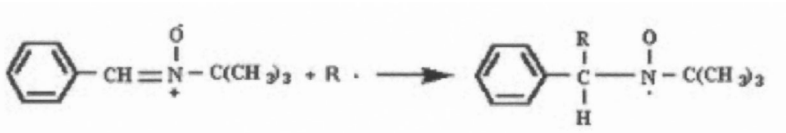

Scheme 1 *Spin-trapping, showing the conversion of a reactive radical* ($R^{\cdot}$) *to a stable nitroxide radical by reaction with the spin-trap (PBN).*

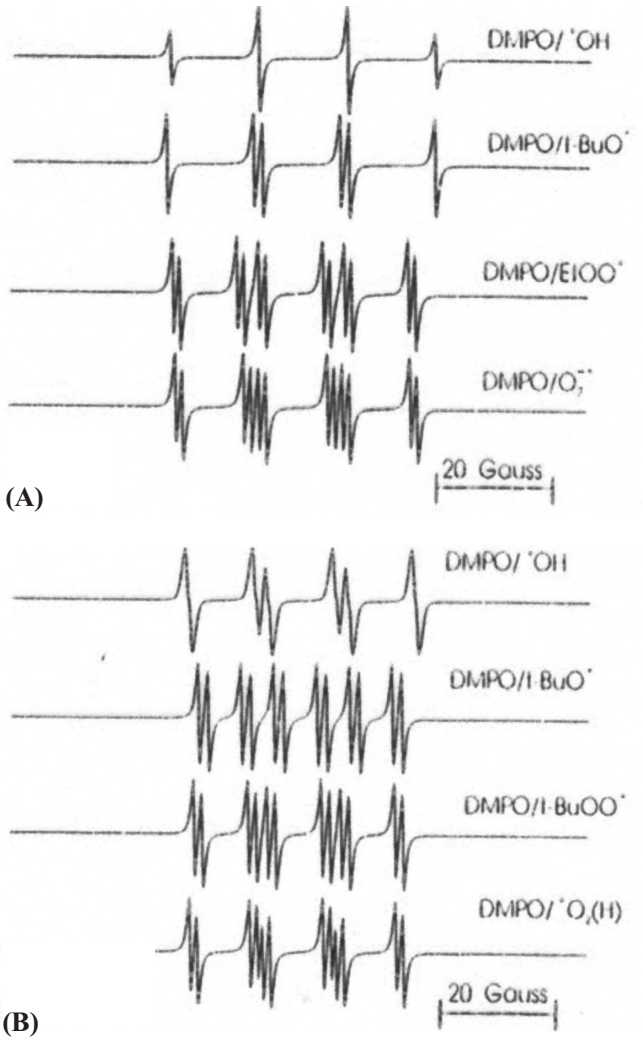

Figure 8 *Spin-trapping of various radicals with the spin-trap DMPO. Spectra shown in series* **(A)** *are measured in aqueous solution abnd those in* **(B)** *in a benzene-toluene mixture. Reproduced from ref. 9, with permission.*

named[9] nitroxides, nitroxyls, aminoxyls; nitroxide radicals, nitroxyl radicals, aminoxyl radicals, and in the context of spin-trapping, collectively, as ''spin-adducts''. Many other materials[10] have been evaluated as potential spin-traps, including thiones, quinones, thioquinones and nitrile-oxides, but their use is very limited, and they almost never feature in biology.

As free radicals, nitroxides are remarkable, since they are indeed stable and have relatively long lifetimes; ranging from minutes to years! Indeed, nitroxides may be bought from chemical suppliers as stable liquids and solids – usually red to orange in colour – for their use as spin-labels and spin-probes. As we have already noted in regard to the difficulty in detecting them by ESR, most radicals are very reactive and short lived; therefore, this unusual feature of nitroxide radicals begs explanation. That many nitroxides can be isolated as liquids or solids, *i.e.* in pure form, demonstrates that they do not dimerise, hence there is no overriding benefit in energy in forming the O—O bond, as in the hypothetical product $R_2N—O—O—NR_2$. In contrast, $HO^{\bullet}$ radicals dimerise in solution at the diffusion-controlled limit, *i.e.* as soon as they meet one another, since by doing so they gain *ca* 50 kcal/mol from the energy released in forming the HO—OH bond. The energy of the O—O bond in all dialkyl peroxides (RO—OR) is smaller, and nearly constant, at *ca* 35 kcal/mol, and more complex reactions occur between alkoxyl radicals ($RO^{\bullet}$) in addition to simple dimerisation[7]. The electronic structure of a nitroxide is more complex than that of an alkoxyl radical, however, and the unpaired electron is delocalised between both nitrogen and oxygen atoms, with only *ca* 50% of it residing on the oxygen atom[10]. This leads to an overall π-bond order of roughly one-half, and a stabilisation energy of *ca* 30 kcal/mol. It is immediately clear that the potential acquisition of *ca* 35 kcal/mol in forming an O—O bond between two nitroxides is far outweighed by the inherent combined loss of 2×30 kcal/mol from the stabilisation energy of the initial two nitroxide molecules. Thus there is little incentive for dimerisation.

The above effect confers long lifetimes to nitroxides without β-hydrogen atoms, such as are most frequently used as spin-labels and spin-probes. However, when this structural feature is present, nitroxides may undergo disproportionation reactions, at various rates depending on the precise type of nitroxide, but sufficiently to limit the lifetimes of spin-adducts in spin-trapping experiments[10]. In biological media, enzymatic processes can in any case oxidise or reduce the nitroxide (respectively *via* removal or addition of a

single electron), and nitroxides will react rapidly with reactive radicals of the ROI (ROS) kind (*vide supra*), such as are implicit to cellular processes. As we see later, these latter properties of nitroxides may be put to use both in studies of cellular metabolism[11] and in the amelioration of free radical induced injury during clinical radiation treatment[12].

4.2 Types of spin-trap

The choice of spin-trap is an important factor in determining the success of a spin-trapping experiment, and the kind of information that it may reveal. There is certainly no such thing as an ''ideal'' spin-trap, and judicious selection of particular features, such as solubility, steric aspects, stability of the spin-adduct, and specificity of the trap for particular radicals is prerequisite; hence there are very many molecules which have found application as spin-traps in differing situations. As noted above, nitrone and nitroso compounds are those most commonly used as spin-traps, and almost entirely so in biological media.

4.2.1 Nitroso compounds

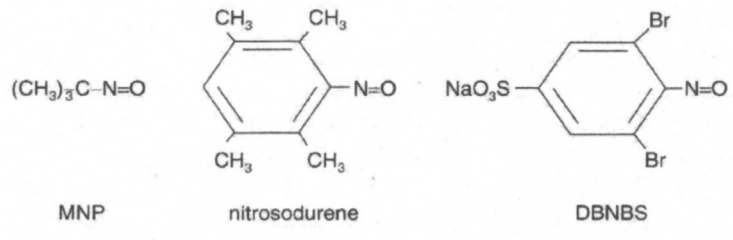

Scheme 2 *Molecular structures of some commonly used nitroso spin-traps.*

Such compounds in common use as spin-traps are: 2-methyl-2-nitrosopropane (MNP) [also called *tert*-nitroso-butane (TNB) in the older literature], 3,5-dibromo-4-nitrosobenzenesulfonate (DBNBS), 2,3,5,6-tetramethylnitrosobenzene [or nitrosodurene (ND)], and 2,4,6-tri-*tert*-butylnitrosobenzene (TBN). The main advantage of nitroso spin-traps is that the radical adds directly to the nitrogen atom, so placing its magnetic nuclei closer to a position of high spin-density than is the case with nitrone traps (Section 3.2.2): this increases the likelihood of success when trying to identify unknown radicals formed in a particular system, or at least in distinguishing between known (or guessed) possibilities[10,13].

The nitroso spin-trap most often used in studies of biological systems is DBNBS, since it is (as its Na^+ salt) both water soluble, and less sensitive to light than are the other nitroso spin-traps[13]. MNP exists in pure form as a dimer, but which dissociates in solution, and while the dimer form of DBNBS also exists, sufficient of the monomer remains to provide an effective spin-trap. However, in the presence of cell cultures and red blood cells, spin-adducts of DBNBS have been shown to undergo rapid decay, and the trap also can give rise to artefact signals under these conditions[14], from which unwary conclusions might be drawn.

4.2.2 Nitrone compounds

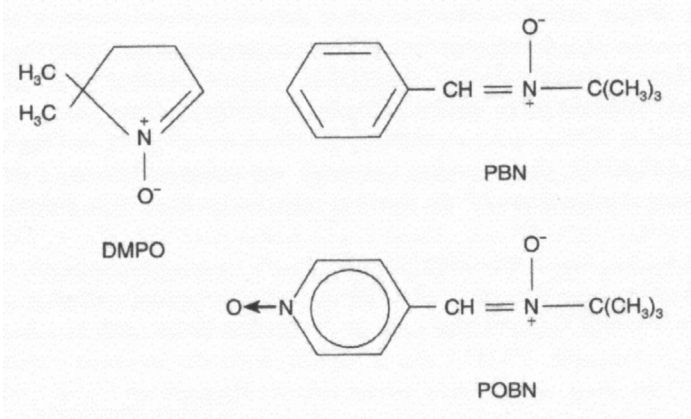

Scheme 3 *Molecular structures of some commonly used nitrone spin-traps.*

There have been a number of nitrone compounds reported as spin-traps, of which the most commonly used are: α-phenyl-N-*tert*-butylnitrone (PBN), α-(4-pyridyl-1-oxide)-N-*tert*-butylnitrone (POBN) and 5,5-dimethyl-1-pyrroline-N-oxide (DMPO). Nitrones are now largely superseding nitroso spin-traps for use in biological media, in consequence of their greater stability, greater water solubility, insensitivity to inadvertent photolysis, greater robustness of their spin-adducts and other properties which, overall, lead to more reliable results[13,15]. When a reactive radical is spin-trapped with a nitrone, the radical adds to a carbon atom adjacent to the nitrogen atom, rather than to the nitrogen atom itself, as occurs with a nitroso spin-trap. This means that, unless isotopic substitution is employed, *e.g.* using a ^{13}C label in the radical $R_3^{13}C^{\bullet}$, only the ^{14}N nucleus and the single β-proton, as was originally present in the spin-trap itself, gives rise to any splitting; consequently, there is

little direct information available regarding the nuclei inherent in the radical itself and so scant clue as to its identity. While these couplings vary to some extent, according to the steric bulk and electronic influence of the trapped radical, the variations are small and cannot, in general, be used with much assurance for its identification. An exception to this is found for adducts of the cyclic spin-trap, DMPO[16], since the unique β-proton is very sensitive to the nature of the trapped radical; particularly to whether the radical is sulfur, oxygen or carbon-centred. While it is hard to distinguish between different radicals within a given series, *e.g.* $RS^{\bullet}$, $RO^{\bullet}$, $ROO^{\bullet}$, ($HOO^{\bullet}$), $R_3C^{\bullet}$, *etc.*, the mere identification of a specific *type* of radical being produced is often invaluable information in mechanistic investigations.

The coupling constants have been measured for thousands of spin-adducts, of different radicals with different spin-traps, of which around 10,000 sets are available *via* the internet, from the Spin Trap Data Base, maintained at the NIEHS (National Institute of Environmental Health Sciences) in the USA (http://epr.niehs.-nih.gov/cgi-bin/stdb); this is also accessible from a mirror site, at Bristol University (http://mole.chm.bris.ac.uk/cgi-bin/stdb). The codes used in this database are a little idiosyncratic, but one soon gets used to them. Otherwise, the essential first step is to ensure that when comparing coupling constants between different spin-adducts, they have been measured in the *same* solvent, *e.g.* there is no point trying to compare an aqueous medium with ethanol or with acetonitrile. This is because coupling constants are always enhanced in more polar media, particularly water (see Figure 8 spectra). Thus forewarned, inspection of the data for coupling constants in a chosen medium across the various types of trapped radical reveals that the unique β-proton coupling in DMPO spin-adducts takes a very narrow range of values for each set of trapped radicals; the influence of various substituents (R), as in the series' listed above, being very small. Hence specific radicals cannot usually be identified, but radicals of a given functional type can. In water solution, the couplings remain close to the following values for each type of radical: $R_3C^{\bullet}$ (23 G); $^{\bullet}CO_2^-$ (19 G); $RS^{\bullet}$ (17 G); $ROO^{\bullet}$ or $HOO^{\bullet}$ (11 G); $HO^{\bullet}$ (15 G); $RO^{\bullet}$ (7 G). The $H^{\bullet}$ atom adduct of DMPO shows a coupling of 23 G, similar to that for $R_3C^{\bullet}$ adducts, but of course, the splitting pattern is a group of three lines (of 1 : 2 : 1 intensity), since there are now two equivalent protons present. The general trend is for more strongly electron withdrawing groups to cause a reduction in the β-proton coupling in DMPO spin-adducts. It is an instructive exercise to peruse the database for

coupling constants outlying from these values, for various assignments of trapped-radicals, which in most cases must merit revision both of the assignment and the proposed mechanism operating in the system under investigation.

4.3 Problems and artefacts of spin-trapping

In an ideal situation, a spin-trap would react only with reactive radicals produced independently of it, to form long-lived spin-adducts, which can be identified by ESR. However, as there is no ideal spin-trap, ideal situations are less commonly approached than we might wish. Nitroso and nitrone compounds, particularly, possess alternative reactivities which can lead to apparent ''spin-adducts'', of ''radicals'' that are not produced ''free'' in the system being investigated[17]. We deal later with the metabolic transformation of nitroxides, principally by enzyme processes, in cells (Section 8.1), but similar kinds of process may modify spin-traps too, such that nitroxides are in fact created: those steps most commonly involved, may be summarised in Eqns (5)–(8):

$$\text{Real spin} - \text{trapping}: \ R^{\bullet} + ST \rightarrow R - ST^{\bullet} \tag{5}$$

$$\text{Oxidation; nucleophilic addition}: \ ST - e^{-} \rightarrow ST^{+\cdot} \rightarrow R - ST^{\bullet} \tag{6}$$

$$\text{Nucleophilic addition; oxidation}: \ ST + R^{-} \rightarrow ST - R^{-} \rightarrow R - ST^{\bullet} \tag{7}$$

$$\text{Reduction; protonation}: \ ST + e^{-} \rightarrow ST^{-\cdot} \rightarrow R - ST^{\bullet} \tag{8}$$

In Eqns (5)–(8) the formal (overall) event is the addition of the group (R) along with an unpaired electron (e-) to the spin-trap (ST), leading to a spin-adduct $R - ST^{\bullet}$. It is, however, only the step represented in [Eqn (5)] which implicates the actual involvement of radicals in a given system; all other steps (6)–(8) being artifacts[17]. Of those most important is the step [Eqn (6)] which leads to the apparent adduct of the spin-trap with the $^{\bullet}OH$ radical, but the actual mechanism is simply that of oxidation of the spin-trap, followed by ''hydration'' in an aqueous biological medium [Eqn (9)]:

$$ST - e^{-} \rightarrow ST^{+\cdot}; \ ST^{+\cdot} + H_2O \rightarrow HO - ST^{\bullet} + H^{+} \tag{9}$$

This leads to the false conclusion that ''free'' $^{\bullet}OH$ radicals are present; misleading indeed, in view of the ubiquitous implication of $^{\bullet}OH$ as a major deleterious agent in ''biology''. Accordingly, various cases of incorrect interpretation have been occasioned in the use of spin-trapping methods in biological systems, and, in

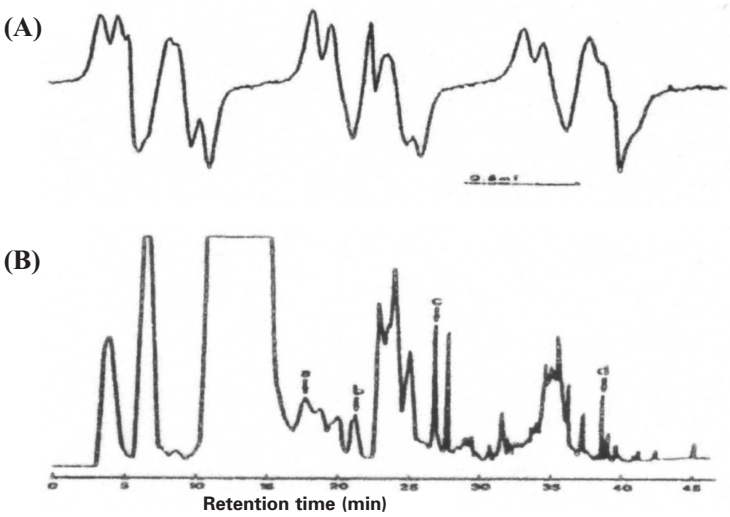

Figure 9 **(A)** ESR spectrum recorded following exposure of aqueous solution of cytidine to x-rays. **(B)** Mixture passed through HPLC column.

overview[15], their majority arise from: (1) molecular changes in the spin-trap itself, which may be due to non-radical, otherwise chemical, photochemical, and mostly enzymatic interventions; physical (and chemical) interruptions of the system under investigation by the spin-trap or its spin-adducts and other products undetectable to ESR; (2) faults inherent to the chemistry of the spin-trap (of the kind summarised in Eqns (6)–(8) which lead to false ''spin-adducts'', as described above; (3) implicit interactions between the spin-trap and its environment in a particular investigation (as an example, it has been discovered only recently that some disposable plastic syringes can contaminate organic solutions of biological extract with a stable nitroxide radical!)[18]. In short, the whole affair of spin-trapping begins to appear as a ''mine-field'', and is indeed well described as such; however, as in crossing a field of ''mines'', careful negotiation can bring a safe and worthwhile outcome!

It is important that such possible events should be anticipated from whatever knowledge is available of the chemistry of the system: in a real biological system this is a difficult task, but our awareness of the properties of such enzyme families (*e.g.* P450) as are implicit to particular tissues or their extracts, *i.e.* in redox reactions [summarised in Eqns (6)–(8) might bring our guard to bear. The identification of a given ''radical (spin) adduct'' should

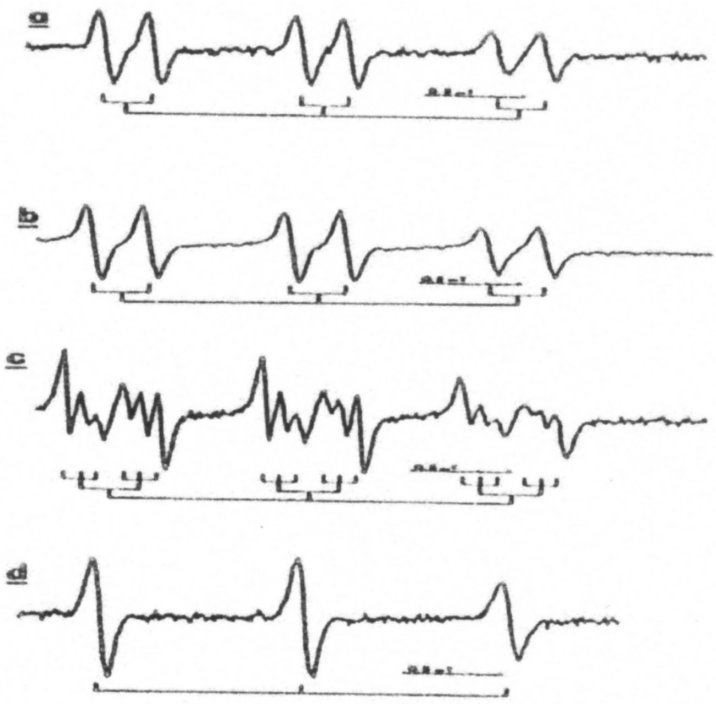

Figure 10 *ESR spectra recorded from the four components marked in Figure 9b, showing individual trapped radicals. It is the overlap of these spectra in Figure 9a that causes the broad lines and makes the spectrum impossible to analyse with any degree of certainty. The individual radical species may be identified from these "separated" spectra.*

not rest entirely upon the measurement of its coupling constants (though, as indicated above, these are surely helpful in the task). As Towner[15] has recently pointed out, there are various approaches that may be used to ensure the correctness of a structural assignment of a radical being formed in a particular system, which include: (1) oxidation of an appropriate secondary amine precursor of the imputed nitroxide [Eqn (10)];

$$R_2NH \rightarrow R_2N - O^{\bullet} \qquad (10)$$

(2) if the signal is absent or very weak, oxidation of the medium, *e.g.* with ferricyanide, to render visible any spin-adduct that has been reduced metabolically to its hydroxylamine form, to enhance the signal-intensity; (3) since no spin-trap is an ideal one, as we maintain, to use various different traps, and compare their results; (4) isotopic substitution, *e.g.* by ^{13}C, ^{15}N, ^{2}H, in the radical

precursor, to compare the ESR splitting patterns and coupling constants, and to determine those atoms from the precursor which have found their way into the particular spin-adduct; (5) similar isotopic substitution in the spin-trap itself, thus introducing magnetically sensitive features of the spin-adduct which vary according to the type of the radical that is trapped; (6) generation of the given radical from different sources, to confirm its appropriate set of coupling constants when trapped as the adduct of a given spin-trap; (7) comprehensive spectral simulation of the ESR spectrum, using all hyperfine components of all possible radicals in their possible relative contributions to a system; (8), in assistance to item (7), when a mixture of spin-adducts is formed in a given system, if they are sufficiently stable, HPLC[19,20] may be used to separate them (Figure 9) prior to an analysis of their individual components by ESR (Figure 10). In conclusion, spin-trapping can provide a wealth of information when done systematically and with care, but is fraught with pitfalls into which the unwary might stumble.

4.4 In-vivo *spin-trapping*

Since spin-trapping accumulates a signal from radical species formed in a system, over time, it is well-placed for the investigation of radical intermediacy in the mechanism of metabolic processes, particularly in regard to toxicology. This is partly because the rates of production of free radicals in biological media are intrinsically low, compared to chemical systems, and also, that water, with its high dielectric constant (relative permitivity) is the worst common solvent for ESR studies, since it limits the sample size to capillaries or flat-cells, placing further demands on sensitivity. There are several recent reviews available, which are concerned with both *in vivo* and *in vitro* aspects of spin-trapping, and which also address specific effects of spin-traps upon enzymes, and more ubiquitous troubles of spin-trapping such as artefacts (see above). In the majority of biological systems, nitroso compounds such as MNP and nitrosobenzene have proved highly toxic at the concentrations required for effective spin-trapping, and their spin-adducts appear rather prone to metabolic reduction. Therefore, all *in-vivo* spin-trapping experiments, to date, have utilised nitrone compounds as spin-traps, which suffer less from these disadvantages.

Mason has enumerated[21] various considerations to be made in the planning and interpretation of *in-vivo* spin-trapping experiments, some of which are reminiscent of those listed above, but are in particular reference to the properties of biological media:

(1) Will the spin-trap participate in reactions other than those with the radical generated in the experiment? Cytochrome P450 inhibition by spin-traps? Are there any pharmacological effects unrelated to spin-trapping?
(2) How readily can the spectrum be interpreted and the structure of the trapped radical be determined? A more specific aspect of this question is the availability of isotopically labelled (^{13}C, ^{2}H, ^{17}O, ^{33}S, *etc*.) compounds or the existence of an independent synthesis of the radical adduct for proof of structure.
(3) How fast is the spin-trapping reaction, and how stable are the radical adducts that are formed? In general, aromatic radical cations and radical anions are not spin-trapped.
(4) Does the appearance of a radical adduct signify a major reaction pathway, or can it be (from) a minor side reaction? Even a minor pathway can have toxicological significance.

In the very first *in-vivo* experiment[22], the spin-trap PBN and carbon tetrachloride were administered to a rat through a stomach tube. After two hours, a Folch extraction was made on its liver and an ESR spectrum was recorded, which suggested the formation of the $^{\bullet}CCl_3$ PBN spin-adduct. Since there is no observable splitting from the $^{35/37}Cl$ nuclei, and 99% of the carbon isotopes are magnetically inactive (^{13}C, with spin $I = \frac{1}{2}$, being in only 1% of natural abundance), the identity of this species was subsequently confirmed using $^{13}CCl_4$, since coupling of the unpaired electron to the ^{13}C nucleus of a trapped $^{\bullet}{}^{13}CCl_3$ radical caused the splitting of all features present in the original ^{12}C adduct into two additional lines.

This was a key experiment, since it settled a lively controversy which illustrates some of the problems encountered in assigning spin-adducts to particular trapped-radicals. It turns out that, in the *in vivo* CCl_4/PBN trapping experiment referred to above, there are a number of adducts formed simultaneously, but the $^{\bullet}CCl_3$/PBN adduct is the only one extracted into chloroform. This underlines one limitation in the procedure of extracting tissue into methanol/chloroform; that only non-polar adducts are ultimately detected. Radical adducts of radical ions, of charged biological molecules, *e.g*. glutathione, or of charged macromolecules such as proteins or DNA will not be extracted and are thus undetectable. This is also an appropriate point to mention *ex-vivo* spin-trapping[23], in which subsequent (chemical) processing of a sample generated *in-vivo* is required, or is advantageous, in the detection of spin-adducts produced during metabolic processes: as a very simple example, the mere bubbling of an extract with oxygen is often sufficient to re-

oxidise hydroxylamines, formed by cellular reduction of the initial nitroxide spin-adducts, back to the originally formed spin-adducts, so that they may be once again visible to ESR. Subsequent removal of oxygen from the solutions with nitrogen gas aids sensitivity, since it reduces the widths of the spectral lines and so increases their intensity; oxygen is paramagnetic, and broadens the lines through Heisenberg-exchange.

The chloroform layer in a Folch extract may often contain sufficient water that tuning of a sample contained in a standard 3 mm diameter ESR tube in the microwave cavity, is not possible, due to dielectric losses, unless the layer is first dried, *e.g.* with anhydrous sodium sulfate, as mentioned above. Mason and his coworkers have managed to circumvent many of the problems now mentioned, by examining the biological fluids (urine, bile, blood or blood-plasma) directly, using a flat-cell of 17 mm cross-section, which presents a far smaller cross-section (*ca* 0.6 mm) to the electric component of the microwave radiation (which is the source of dielectric loss), while maintaining the greatest possible sample volume in the active region of the cavity. Since the solubility of oxygen in water is quite low (*ca* 250 μM O_2 in equilibrium with air), deoxygenation is not normally required, although the intensity of very sharp lines will be so enhanced[21].

In an attempt to improve the resolution of spectra so to facilitate the identification of spin-adducts, and hence their trapped radicals, the use of PBN partially substituted with deuterium atoms was introduced by Janzen[24]. The compound lends sharper lines to its spin-adducts, and can allow additional coupling constants from the trapped radical to be resolved. As an example of its success, we may refer to a study of the bile collected from rats treated with the anaesthetic halothane ($CF_3CHBrCl$) along with the deuterated PBN[25]. This anaesthetic has been implicated in human metabolic hepatotoxicity, which is experienced in a mild form by as many as 20% of patients to whom it has been administered. The mechanism is believed to involve a reductive debromination step, leading to carbon-centred, $CF_3CHCl^{\bullet}$, radicals. In order to simulate the resulting ESR spectrum, a composite of the simulations for two radical-adducts was required. Therefore, one might quite reasonably conclude that two separate radicals have been formed from halothane, whereas in fact, there is only a single species trapped, the expected $CF_3CHCl^{\bullet}$, radical. The solution to this apparent paradox is that in its radical adduct with PBN, both the 2-C carbon atom derived from halothane and the carbon atom adjacent to the phenyl group are chiral. Thus, two distinct diastereoisomers

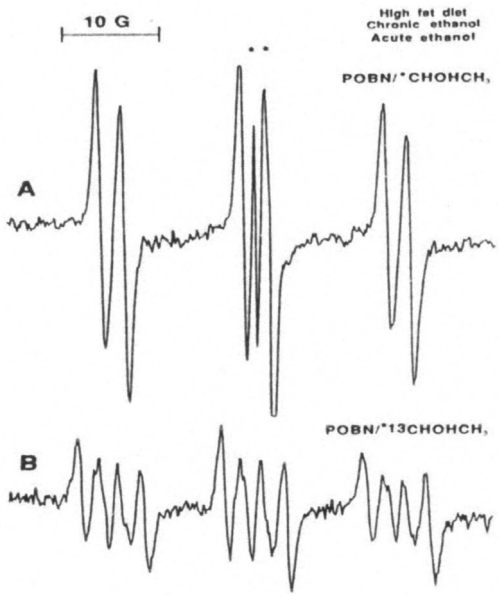

Figure 11 *ESR spectra recorded from bile taken from alcohol deficient deermice* **(A)** *fed with acute ethanol and the spin-trap POBN and* **(B)** *as in* **(A)** *but using the isotopically-labelled ethanol* $CH_3{}^{13}CH_2OH$*, showing an extra "doublet" coupling from the* ^{13}C *nucleus and that the metabolite radical is* $CH_3{}^{13}C{\cdot}HOH$*. The additional two lines marked in (A) are from the ascorbate radical. Reproduced from ref. 9, with permission.*

of the radical adduct are possible and will give two distinct spectra, even thought there is only one radical species trapped. The identical origin of these spectra was confirmed by using halothane which has been ^{13}C labelled at the 2-C position, when an additional two-line splitting resulted in both of them[25].

As a final example, we consider a study of alcohol metabolism, using *in vivo* ESR. It has been known since antiquity that chronic abuse of ethanol results in widespread pathological changes, particularly in the liver (''fatty'' liver). These changes were first attributed to lipid peroxidation by Di Luzio[26], and Slater[27] proposed that the metabolism of ethanol might involve the production of carbon-centred radicals, which could initiate lipid-peroxidation. Using the spin-trap POBN, an ESR spectrum was recorded from bile taken from the gall-bladders of six deermice which had been chronically fed with an ethanol-rich, high-fat diet, and then an acute dose of ethanol (rather forcing conditions), showed a central signal from ascorbyl radicals, superimposed on a six-line pattern which is characteristic of the spin-adducts of many types of carbon centred

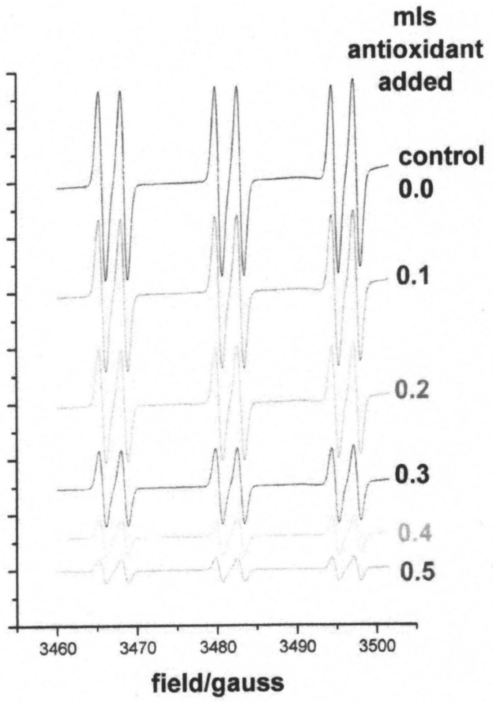

Figure 12 *Reduction in intensity of peak from spin-adduct of $CH_3^{\bullet}$ radicals and PBN by increasing concentration of an antioxidant. The higher the concentration of the antioxidant the more of the $CH_3^{\bullet}$ radicals are scavenged.*

radical, and is not definitive [Figure 11 (A)]. In order to confirm that the radical responsible for this signal was indeed derived from the ethanol, a ^{13}C label was introduced in the form of $CH_3{}^{13}CH_2OH$. This resulted in a splitting of each of the original six-lines into two more [Figure 11 (B)], thus confirming that the adduct is POBN/$CH_3{}^{13}CHOH^{\bullet}$, and that $CH_3{}^{13}CHOH^{\bullet}$ radicals are indeed a product of ethanol metabolism[28].

4.5 Competitive spin-trapping: measurement of antioxidant efficiencies

There is considerable current interest in determining the relative scavenging ability of antioxidants for biologically important radicals. These radicals may be generated in model systems, and in order to generate particular types of radical, the following reagent mixtures may be used:

Superoxide (xanthine/xanthine oxidase);

Peroxyl radicals (AAPH; (2,2′-azobis(2-amidinopropane) hydrochloride); Hydroxyl radicals (Fe(II)chelate or Fe(III)chelate + reductant, hydrogen peroxide); Alkyl ($CH_3^{\bullet}$) radicals (Fe(II)chelate or Fe(III)chelate + reductant, hydrogen peroxide, dimethylsulfoxide).

The essential procedure is to add a spin-trap (*e.g*. PBN, DMPO) to one of the above model-systems, and to determine the intensity of the spin-adduct in the absence of an antioxidant. The antioxidant is then added at known concentration, and competes kinetically with the spin-trap. From the relative diminution of the spin-adduct signal (Figure 12), a relative ordering of antioxidant efficiencies may be established within a series of compounds.

It is important to be aware that not all of these model systems generate 100% of one radical species, and that the essential chemistry of the system may be affected by the presence of the spin-trap or of the antioxidant. To check for the latter phenomena, more than one spin-trap should be tried and a series of antioxidants investigated, initially varying the order of mixing the reagents with the antioxidant solution (*i.e*. if the underlying chemistry is being affected, the intensity of the spin-adduct signal should change).

In one study[29], a mixture of hydrogen peroxide, $FeSO_4$ and DMSO was employed, using PBN as the spin-trap. $^{\bullet}OH$ radicals were produced by the Fenton reaction, which are scavenged by DMSO, to give $^{\bullet}CH_3$ radicals, which are either trapped by PBN or react with an added antioxidant. For a series of flavonoid antioxidants at a concentration of 4.8 mM, the following relative intensities of the $^{\bullet}CH_3$-PBN spin-adduct signal were recorded:

Antioxidant	Percentage of control ESR signal
Caffeic acid	8
o-Coumarin	13
6,7-Dihydroxy-4-methylcoumarin	18
Catechin	19
Scopoletin	112

The relative rates for the reaction of $^{\bullet}CH_3$ radicals with the antioxidants may be deduced from these data, with respect to the spin-trap. It is interesting that the rates do not follow a simple statistical factor, *i.e*. are not merely proportional to the number of hydroxyl groups present, since the rates are nearly identical for 6,7-dihydroxy-4-methylcoumarin, with two hydroxyl groups, and catechin with four (bound to aromatic rings; the fifth OH group is attached to an alkyl ring and will not form a stabilised radical). More strikingly, scopoletin shows an enhancement in

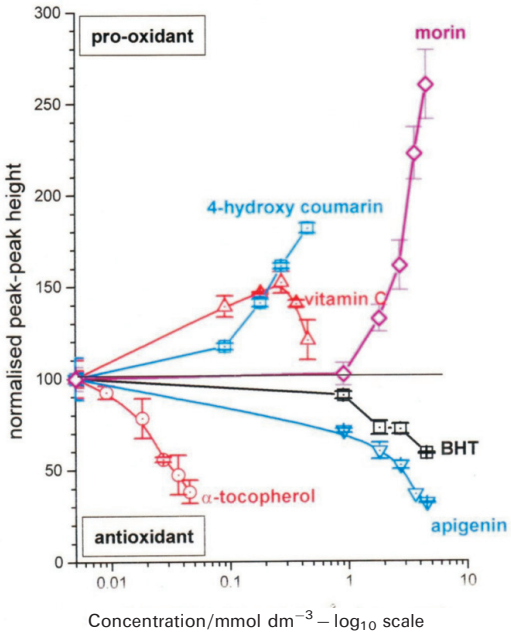

Figure 13 *Effect on intensity of peak from spin-adduct of $CH_3^{\bullet}$ radicals and PBN according to increasing concentrations of "antioxidants". The horizontal line is the "normal". Below it, the substances are displaying expected* antioxidant *behaviour. Above the line, the substances are showing the opposite,* pro-oxidant *behaviour.*

the signal intensity, and is therefore behaving as a *pro*-oxidant. A study was made of the effect of concentration on the activity of catechin: at 4.8 mM concentration, it is strongly antioxidant, but the effect weakens at lower concentration, until at 3.6 mM, there is apparently no effect; at lower concentrations, however, a marked pro-oxidant behaviour is evident, and at 0.5 mM, the ESR signal is enhanced by 400% from the control!

In order to explore the aspect of antioxidant *versus* pro-oxidant activities for phenols and polyphenols (ArOH) in more detail using ESR, a more structurally diverse series of compounds was investigated[30]. Although it might be thought ideal to look at the relative rates of reaction for $^{\bullet}OH$ radicals, generated using a Fenton system, with antioxidants, almost all such reactions proceed at the diffusion controlled rate and so little discrimination is possible between different antioxidant (pro-oxidant) activities. Hence, DMSO was employed to serve both as the solvent and as a radical scavenger, which generates $^{\bullet}CH_3$ radicals [Eqn (11)] which react with phenols [Eqn (12)] more slowly than $^{\bullet}OH$ radicals by a factor of about *ten*,

thus enabling far better discrimination in establishing an order of reactivity types:

$$^{\bullet}OH + (CH_3)_2SO \rightarrow CH_3SOOH + {}^{\bullet}CH_3 \qquad (11)$$

$$^{\bullet}CH_3 + ArOH \rightarrow ArO^{\bullet} + CH_4 \qquad \text{(SLOWER)}. \qquad (12)$$

The spin-trap, PBN, is also introduced at known concentration, and by varying the ArOH concentration, the rate constant for the reaction of $^{\bullet}CH_3$ with the antioxidant may be determined relative to the spin-trapping rate. For genuine antioxidant behaviour, the simplest case is when the ESR signal from the spin-adduct has been reduced to 50%: this means that the $^{\bullet}CH_3$ radicals are reacting at an equal rate with both PBN and ArOH [Eqn (13)].

$$k_1[PBN] = k_2[ArOH] \qquad (13)$$

[Since both concentrations of [PBN] and [ArOH] are known, the relative rate constants k_1/k_2 can be determined. If k_1 is available, say, from a pulse-radiolysis study, k_2 can be evaluated]. Since these compounds display widely different reactivities, comparison of all the data sets is facilitated by plotting the concentration on a logarithmic scale (Figure 13). A ''100% normal'' line is included which represents the intensity of the signal recorded in the presence of the spin-trap alone; therefore, all points which lie below the line reflect antioxidant behaviour, and those above it indicate that the compound is acting as a pro-oxidant. We see that α-tocopherol, apigenin and ''butylated hydroxy-toluene'' (BHT) all display antioxidant activity, each within its concentration range, while 4-hydroxycoumarin and morin appear to be profoundly pro-oxidant. Vitamin C is curious in its behaviour, since its pro-oxidancy appears to go through a maximum. We believe that these compounds are able to act as pro-oxidants by their reduction of Fe^{3+} back to Fe^{2+}, so prompting further Fenton chemistry and $^{\bullet}OH$ radical generation. In support of this, we note that morin and apigenin show almost diametrically opposed behaviour, and yet their structures are very similar: it seems likely that the presence of the OH group adjacent to the C═O group in morin assists this compound as a chelator, and facilitates the reduction of a ''coordinated'' Fe^{3+}.

The concentration affects found for catechin are interesting. One explanation is that, at low concentrations, radical scavenging by the antioxidant is less efficient, whose principal role then becomes the regeneration of Fe^{2+}. The biological implications of these observations are interesting: does it mean that a too low intake of some

antioxidants in the diet may do more harm than good? However, we must recall that this is a model system, and that it contains free Fe^{2+} and Fe^{3+}; in real biological systems, iron is mainly sequestered in proteins such as ferritin and haemosiderin, but is known to become toxic when released by de-complexing agents. Indeed, many materials are toxic through an indirect route, *e.g.* paraquat, which generates high levels of superoxide in the lungs, through redox cycling, and alcohol, which encourages the expression of cytochrome P450 enzymes, which are known to activate other toxic materials into more virulent forms.

4.6 Detection of "oxidising species" in human biological fluids

The spin-trap, 3,5-dibromo-4-nitrosobenzene sulfonate (DBNBS) has been used to detect the presence of an oxidising species, both in the plasma of patients suffering from renal failure receiving haemodialysis[31], and in the synovial tissue from patients undergoing primary total knee joint replacement[32]. The resulting ESR spectrum consists of three hyperfine lines of approximately equal intensity, showing $a(^{14}N) = 13.2\,G$, and $g = 2.00832$, and was ascribed to the DBNBS radical cation ($DBNBS^{+\cdot}$). The formation of this paramagnetic species was suggested by Nazhat *et al*., by the horseradish peroxidase catalysed oxidation of DBNBS by H_2O_2;[33] however, Ichimori *et al*.[14] pointed out that the same ESR signal had also been observed in other systems: the horseradish peroxidase catalysed oxidation of sulfite by H_2O_2;[34,35] the xanthine/xanthine oxidase system containing dimethyl sulfoxide;[33,36] the Fenton reaction system including H_2O_2 and Fe^{3+};[37] the oxidation of selenite by Ce^{4+} ions[38]. These workers assigned the radical species formed in all of these experiments to the DBNBS adduct of the $SO_3^{-\cdot}$ radical ($DBNBS - SO_3^{-\cdot}$). In a detailed study[39], using DBNBS isotopically substituted either individually with ^2H or ^{15}N, or as doubly labelled with both isotopes, it was shown that an additional triplet splitting of 0.6 G was resolved in the spectrum of the authentic $DBNBS - SO_3^{-\cdot}$ radical, which arises from coupling to the two protons, which are ''ortho'' to the nitroso group. Since this was absent in the spectrum recorded from DBNBS in the presence of the biological fluids, it is proposed that the radical species are different, and that, in the latter media, it is $DBNBS^{+}$ that is formed.

Some comparison may be drawn, however, with the ESR spectrum recorded from authentic nitrosobenzene radical cations

($PhNO^{+\cdot}$),[40] as isolated in a solid $CFCl_3$ matrix at 77 K. Since the radical cations are immobilised on the spectroscopic timescale under these conditions, the isotropic $a(^{14}N)$ coupling must be extracted by averaging the ''parallel'' and ''perpendicular'' values, but it amounts to *ca* 33 G. Since this is *by far* greater than that detected in the above biological media, it casts grave doubt upon the interpretation that it is $DBNBS^{+\cdot}$ that is formed therein. It is conceivable that $DBNBS^{+\cdot}$ is formed in a π-electronic state, as opposed to the σ-state which is clearly adopted by $PhNO^{+\cdot}$, given its large coupling, but one would expect the ^{14}N coupling for the π-state actually to be *vanishingly* small. Comparison with the ''spin-trapping'' database ((http://epr.niehs.nih.gov/cgi-bin/stdb) for DBNBS adducts shows, in fact, that a ^{14}N coupling of 13.2 G is typical for genuine spin-adducts of DBNBS (including the species $DBNBS - SO_3^{-\cdot}$, referred to above). I suggest, alternatively, that the radical species is a genuine spin-adduct, perhaps of a *tertiary* radical (hence the lack of additional hyperfine splitting), and one with sufficient size, or interaction with the medium, that the lines are broadened just enough to preclude resolution of the 0.6 G splitting.

DBNBS has also played a role in another important biological controversy: namely regarding the ''spin-trapping'' of nitric oxide (NO).[41] The matter is controversial because NO, being rather unreactive as a free radical, is not actually ''trapped'' in the usual sense of ''spin-trapping''. Although NO reacts with DBNBS to form a stable radical product, which is characterised by a three-line ESR spectrum due to ^{14}N with a splitting of 9.6 G, it has transpired, that this is not the simple DBNBS-NO adduct. Using a two-stage HPLC fractionation, this radical product was isolated from the other components of the reaction mixture, and was identified using fast atom bombardment-mass spectrometery as the dianion, *bis*(2,6-dibromo-4-sulfophenyl)nitroxyl[41]. Further studies[42,43] also indicated that significant quantities of nitrogen (N_2) and nitrite anions (NO_2^-) were formed during the reaction. A possible mechanism consistent with these observations was proposed. The reaction between DBNBS and NO, produced from nitrite anions in acid solution, has been used as a means for measuring nitrite in whole bllod, plasma and synovial fluid taken from rheumatoid arthritis patients, since the height of the low-field line in the resulting *bis*(2,6-dibromo-4-sulfophenyl)nitroxyl spectrum is directly proportional to the nitrite concentration, from 3.0 μM to at least up to *ca* 0.08 mM.

5. Determination of nitric oxide

Nitric oxide (NO) is ubiquitous in biology[44–47], and was named as ''molecule of the year'' by Science Magazine in 1992 because by far the most papers had been published in that year in relation to this species, alone of all other molecules. It is formed from L-arginine by the action of NO synthase. NO is an important messenger molecule for the regulation of immune function and the dilation of blood vessels; it also serves as a neurotransmitter. It is also produced in excess during ischaemia, presumably in an attempt to bring oxygenated blood to sites of oxygen deprivation. NO has also a potential pathological role, being a reactive species, both directly, and more importantly *via* its reaction with the superoxide radical anion to form peroxynitrite, $^{-}$OONO, and peroxynitrous acid, HOONO, especially if the pH is lowered by lactic acidosis. HOONO is particularly dangerous because it can easily cross cell-membranes, and at some later stage may decompose to form $HO^{\cdot}$ radicals and $^{\cdot}NO_2$, or be directly oxidising in itself. Therefore, $HO^{\cdot}$ radicals, or other oxidising species, may be delivered to sensitive sites which otherwise would be protected from them.

Although the presence of an unpaired electron defines NO as a free radical, all attempts to trap it, using conventional nitrone or nitroso spin-traps have been largely fruitless[48]. Alternative strategies have been tried, employing dienes[49,50], and also a photochemically generated derivative of ortho-quinodimethane[51], but these are not really practical as ''traps'', since dienes frequently result in mixtures of nitroxides, and the ortho-quinodimethane is not the major photolytic product of its precursor, 1,1,3,3-tetramethyl-2-indanone, and it is in any case not stable. As a free radical, NO is rather unreactive, but it is a good ligand, and various iron complexes, notably Fe(II)-diethyldithiocarbamate [$Fe(DETC)_3$], are highly efficient traps of NO[43]. In the presence of NO, [$Fe(DETC)_3$] is converted to the stable complex, [$Fe(NO)(DETC)_2$], with an ESR pattern that is characterised by the components, $g_{\|} = 2.02$, $g_{\perp} = 2.035$. In [$Fe(NO)(DETC)_2$], four sulfur ligands chelate the iron aton, which is in the formal oxidation state of $+1$, and protrudes from the base, while the NO ligand occupies the apical site. This complex is paramagnetic by virtue of an unpaired electron which is associated with the d^7 electronic configuration of iron. In some applications, [$Fe(DETC)_3$] is added directly, while in others, as described first, under the heading *specific examples*, the complex may be generated *in situ*.

It is also worth noting that a complex which is commonly referred to as ''nitrosyl-haemoglobin'' is frequently detected in diseased tissue, for example in some cancers and in the diseased synovium[44], as removed from a patient suffering from rheumatoid arthritis in this case during surgery for a knee-replacement. Whether NO is central to the mechanisms which cause these diseases or rather is a consequence of them is unknown; however, the presence of nitrosyl-haemoglobin does appear as symptomatic of diseased tissue.

5.1 Some specific examples.

5.1.1 Quantification of NO in aqueous media, cells and tissues (using an "in situ generated" Fe(DETC)$_3$ complex)

The beauty of this technique, is that the [Fe(DETC)$_3$] complex is generated *in situ* by the reaction between DETC and Fe^{2+} present naturally in yeast, cells or tissue, and merely requires incubation of the sample with the free ligand DETC (diethyldithiocarbamate), without addition of pre-formed [Fe(DETC)$_3$]. The method enables the detection of NO down to 0.05 nmol as present in sample volumes of 0.7 mL. Adaptations of the method described below, have been applied to the detection of NO both in cultured cells and in tissues (vascular tissues and cerebellar slices), and in vascular and other tissues *in vivo*, as is fully described in the literature[45–47]. In all cases, the [Fe(NO)(DETC)$_2$] complex accumulates preferentially in cell membranes.

5.1.2 Aqueous media[43,44]

Both complexes, [Fe(DETC)$_3$], and its product with NO, Fe(NO)(DETC)$_2$, are insoluble in water, and so must be dissolved in a highly dispersed, lipophilic medium. Yeast membranes serve this purpose very well. A suspension of bakers' yeast in Hepes buffer (15 mM, pH 7.5) is first heated in boiling water for half-an-hour, in order to destroy catalase activity and to impair oxygen consumption; it is then incubated with DETC (2.5 mg/mL) for another half-an-hour at 37°C. DETC chelates Zn^{2+} and Cu^{2+}, in addition to Fe^{2+}, all of which are present in yeast; the Cu^{2+} complex is paramagnetic, so contributing to the background signal. However, only the [Fe(DETC)$_3$] complex traps NO, and an aliquot of the yeast suspension is added to the potential NO-producing

solution, to a final yeast concentration of 60 mg/mL. It is found to be advantageous to add solid sodium dithionite to the samples between one and three minutes prior to the conclusion of their incubation; this regenerates the proportion of $[Fe(NO)(DETC)_2]$ which has been oxidised during the procedure, and renders the method overall quantitative.

ESR spectra were recorded from samples of yeast, which had been incubated with DETC under various conditions[43,44]. In a sample that had been incubated both in the absence of NO donors or dithionite treatment, the spectrum was dominated by the $[Cu(NO)(DETC)_2]$ complex, which appear as four lines, since both ^{63}Cu and ^{65}Cu have spin $I = 3/2$, and their couplings are almost identical (the relative abundances of ^{63}Cu and ^{65}Cu are 69.2% and 30.8%, respectively). In the scan-range of the magnetic field over which the $Fe(NO)(DETC)_2$ complex is detected, only the three highest-field lines were visible. The spectrum was recorded from the sample as frozen at $-196°C$ (77 K); in contrast, at $+37°C$, when the sample was liquid, its signal was rendered undetectable by the effect of power-saturation. The features from $[Fe(NO)(DETC)_2]$ were more distinct when NO had been trapped from an aqueous 0.1 mM solution, and when NO had been generated using porcine cerebellar NO synthase. These spectra reveal principal components of $g_{\|} = 2.02$ and $g_{\perp} = 2.035$, with an incompletely resolved triplet pattern on the $g_{\perp}$ feature, due to hyperfine coupling with the ^{14}N nucleus of the trapped NO moiety. At low concentrations of NO, only the third (highest field) hyperfine line of the $g_{\perp}$ feature is not obscured by the signal from the [Cu (NO)$(DETC)_2$] complex, and so may be used to determine the concentration of trapped NO. In the liquid phase, the spectrum from $[Fe(NO)(DETC)_2]$ became isotropic, because the $g_{\|} = 2.02$ and $g_{\perp} = 2.035$ components are averaged by rapid molecular tumbling, and is characterised by an isotropic g-value, $g_{iso} = 2.03$, and an isotropic hyperfine triplet ^{14}N coupling of *ca* 13 G. The ESR signal from $[Fe(NO)(DETC)_2]$ is ''indefinitely'' stable in samples which are stored as frozen at $-196°C$ (77 K), but for 1 h in suspended yeast at 37°C.

5.1.3 Adaptation of trapping NO in an aqueous phase, to an "on-line" method[47]

Given that the $[Fe(NO)(DETC)_2]$ signal *is* stable in suspended yeast samples for at least one-hour, it is possible to determine the rate of production of NO over at least this time-period, and in these media.

Such a determination of the accumulation-rate of NO, over time, may be described as an ''on-line'' measurement. In one experiment, ice-cooled yeast (60 mg/mL), loaded with DETC and suspended in Hepes solution, was mixed with cytosol from porcine cerebellum (1 mg/mL) along with L-arginine and NO synthase cofactors. This ice-cold mixture (which constituted a total final volume of 140 microlitres) was introduced to a long 10 cm), flat, cuvette and the ESR signal from trapped-NO was recorded over 50 minutes, by adjusting the magnetic field to the position of the first low-field triplet line of the $[Fe(NO)(DETC)_2]$ signal. Analysis of this accumulation-curve enables the evaluation of the rate constant for NO formation, which is characteristic of the particular system. Interestingly, Yordanov and his coworkers[52] have applied the methof for the sequential determination of nitrate and nitrite anions in vegetables and fruits through reactions that generate NO from each, which can be detected as the $[Fe(NO)(DETC)_2]$ complex using ESR.

6. Oximetry

The partial pressure of oxygen is one of the key factors in influencing many processes in biology. As the terminal electron acceptor in the electron transport chain, oxygen plays a decisive role in cellular metabolism. Conversion of oxygen to ROI's (reactive oxygen intermediates), *e.g.* $^{\bullet}OH$, $O_2^{-\bullet}$, $HO_2^{\bullet}$, $RO_2^{\bullet}$, $NO^{\bullet}$, H_2O_2, HOONO, and their reactions with cell and tissue components, are now thought to be integral to many diseases, and to the process of aging itself[53]. Nonetheless, means for measuring Oxygen in cells and tissues are lacking, *e.g.* the Clark electrode, fluorescence quenching, O_2 binding to myoglobin and spin-label oximetry are in general useful, but suffer from various limitations when applied to real biological samples. In pioneering work by Swartz and his coworkers[54], several materials have been discovered which contain stable free-radical signals, whose linewidths are sensitive to the concentration of oxygen in their immediate environment. Thus, by introducing such material to the region for investigation, and measuring the ESR spectral linewidths, an accurate determination of the local oxygen concentration can be made. Some of the materials which demonstrate this effect are: lithium phthalocyanine crystals[54], particles of natural charcoals such as fusinite or ''gloxy'',[55] and some synthetic carbon chars[56,57], formed *e.g.* by pyrolysing sucrose. The label ''gloxy'' is derived from the Welsh word for ''coal''–and ''oxy'', to

demonstrate this particular application. India ink, introduced to skin in the form of a ''tattoo'' finds a useful application in that it provides a similarly oxygen-responsive ESR signal, and so, *e.g.* the fall in oxygen concentration following ligation of a limb can be monitored, provided that the sample is not too large to be accommodated within the magnet and resonator of the apparatus (*i.e.* an arm from most people could probably be so examined, but a fairly ''thin'' person would be needed for a leg!). For animals smaller than humans, *e.g.* rats or mice, the whole animal may be included in the ESR spectrometer.

In anticipation of the more widespread use of ESR-oximetry, efforts have been made to discover sources of charcoal, which might be available in reasonable quantities, with optimum ESR properties: a narrow linewidth in the absence of oxygen, a high sensitivity of the linewidth to variations in such oxygen concentrations as may be present in tissue, and that the response and the signal itself should be stable. In one such investigation[58], a total of 34 different kinds of charcoals, routinely available in laboratories, were investigated, only 17 of which comprised the *a priori* requirement of a detectable ESR signal (this an interesting feature since it is often supposed that *all* charcoals contain unpaired electrons); from which eight samples were selected for further study. The difference in linewidth was observed for one sample, a live-mouse, into which 50 microlitres of a coal slurry had been introduced to the gastrocnemius muscle, according to a normal and a restricted blood-flow. The signal is sharper under hypoxic conditions, and from a suitable calibration the oxygen concentration may be determined. The calibration curve was established from *in vitro* measurements, in which about 50 mg of the charcoal powder or its suspension (100 mg/mL) in water is placed in the same region of the spectrometer to be used for the *in vivo* measurements. The responsiveness of three stable charcoals to changes in oxygen concentration incurred by restricting the blood flow in the muscle was determined, and calibration curves were obtained for each charcoal. The charcoal signal was found to be stable for as much as four months, demonstrating the feasibility of long-term studies of oxygen concentrations[58].

In some applications, it is advantageous to use the linewidths in the ESR spectra of nitroxides to probe oxygen concentration. Such measurements may be made in conjunction with studies of metabolism, using nitroxides; so revealing multiple features of a particular biological system. However, a too rapid rate of bioreduction may be a disadvantage, when it is desired to determine the

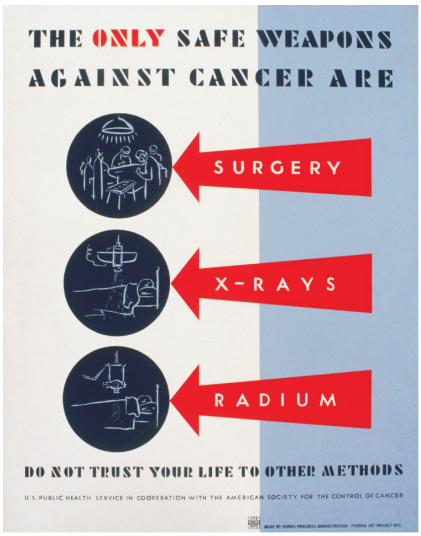

Figure 14 *A 1938 poster claiming only surgery, x-rays and radium as the proper treatments for cancer. Credit Anthony Velonis. http://upload.wikimedia.org/wikipedia/commons/0/0b/Cancer_add-Restored.jpg*

oxygen concentration over a significant time period. One solution is to incorporate the nitroxide into proteinaceous microspheres[59], which may be generated using ultrasound, to retard the reduction process. The procedure has the further positive element that the intrinsic sensitivity of the nitroxide probe to oxygen is increased, since the concentration of oxygen in the ''organic'' microsphere is increased over an aqueous medium.

7. Radiation effects

7.1 Radiation dosimetry

ESR was proposed several years ago as a method for the measurement of radiation dose, and in most cases, L-alanine is the material of choice as a dosimeter, since it possesses a reasonable radiation sensitivity and a very stable free radical signal. It also has excellent properties regarding tissue equivalence and linear dose response, and so it has been recommended by the IAEA for the measurement of high radiation doses[60]. However, the radiation sensitivity of alanine is too low to be applied in dosimetry for medical treatment, *e.g.* in cancer therapy (Figure 14). New materials, which are sensitive in the range 0.5–100 Gy, are needed if ESR is to

become a serious alternative to existing methods of dosimetry, *e.g.* ionisation-chambers, Si-diodes, thermoluminescence or chemical dosimetry such as Fricke solution. The criteria to be met by such materials are: a high radical yield, linearity of the signal intensity with dose, sharp spectral lines and a stable signal over time, at room temperature[61]. Various compounds have been evaluated in this regard, as described below[62].

7.1.1 (Ammonium tartrate, $NH_4^+ \ ^-OOCCH(OH)CH(OH)COO^- \ NH_4^+$)

The ESR spectrum from alanine has a far greater overall width than that from ammonium tartrate, as recorded from both materials following X-irradiation and as recorded at room temperature, while the actual lines are approximately similar and fairly broad: due to hyperfine anisotropy in the alanine derived radical, $CH_3C^{\bullet}HCOO^-$ (mainly from the unique α-proton), and unresolved hyperfine structure in the $NH_4^+ \ ^-OOCC^{\bullet}(OH)CH(OH)COO^- \ NH_4^+$ radical. For ammonium tartrate, the signal intensity measured peak-to-peak was twice as high as the alanine signal, and three-times higher for a sample of ammonium tartrate that had been crystallised from D_2O, which reduces the width and increases its intensity of the spectral line[62]. [This is probably due to substitution of the OH protons by OD deuterons, thus turning the unresolved OH doublet splittings into OD triplets, but with separations smaller by a factor of 6.514].

7.1.2 (2-Methylalanine)

The spectrum recorded from 2-methylalanine consists of seven lines, from the radical $(CH_3)_2C^{\bullet}COO^-$. The lines are relatively narrow, because of the small hyperfine anisotropy associated with β-protons. At a microwave power of 1 mW and a modulation amplitude of 7.25 G, 2-methylalanine has a 70% higher sensitivity than alanine[60].

7.1.3 Formates, $HCOO^-$

In the case of formates, single line spectra were observed in most of the compounds tested. The signal is from the $^{\bullet}CO_2^-$ radical, and in the lithium salt, $HCOO^-Li^+$, the signal intensity was three times that from alanine in the dose range 1 – 10 Gy at a modulation amplitude of 1 G. The signal intensities of samples exposed to the

Figure 15 *The radura logo as required by the US Food and Drug Administration. Credit Euratom. http://en.wikipedia.org/wiki/Radura*

same X-ray dose depended on the type of cation present and increased in the order $Li^+ < NH_4^+$, $Mg^{2+} < Ca^{2+}$. One problem encountered with these compounds as dosimeters is the line-broadening caused by g-anisotropy and unresolved hyperfine structure from the cation[62]. ^{23}Na hyperfine structure was actually resolved for the sodium salt (a quartet of equal intensity lines, since ^{23}Na has nuclear spin $I = \frac{3}{2}$).

7.1.4 Dithionate salts, $S_2O_6^{2-}$

Narrower lines were found for some irradiated dithionate salts, in which the radical formed is $^{\bullet}SO_3^-$. This radical has a nearly isotropic g-value, and all magnetic S and O nuclei are in extremely low natural abundance, hence a narrow single-line spectrum occurs. The peak-to-peak intensities of a series of dithionate salts containing different cations and irradiated to the same dose by X-rays from a 4 MeV linear accelerator increased in the order $NH_4^+ < Cs^+ < Li^+ < Rb^+ < Ba^{2+} < K^+$. The radical yield in the ammonium salt appeared to be far lower than in any of the other compounds, while that in $K_2S_2O_6$ is about ten times that in $Cs_2S_2O_6$; this can be partly explained in terms of different hyperfine interactions with the different cations. A spectrum was recorded from $K_2S_2O_6$ which is of 10 times the intensity of that recorded from alanine following the same X-ray dose, which is very encouraging. However, the material is not ''tissue-matched'', unlike alanine, but from the standpoint of sensitivity, $K_2S_2O_6$ is superior to all other materials so far investigated[62].

7.2 Irradiation of drugs

Radiation has been used for many years as a means for sterilising various materials and devices used in medicine, and is set to become more widespread for the sterilisation of drugs. Active ingredients may be irradiated alone, or in quite complex mixtures[63,64]. As model systems, several amino-acids and one antibiotic, ampicilline acid, were chosen, and were exposed to γ-rays from a 50,000 Ci ^{60}Co source[65]. In ampicilline acid, an unresolved single line spectrum was recorded, which was found to be stable for more than one year. In the amino-acids, more or less complex ESR spectra were recorded, depending on the molecular structure, but which were also stable over storage times of months or years. In the case of alanine, no change was found in the intensity or nature of the signal, even after a period of 2 years, which makes this material suitable as a radiation dosimeter, for measurements of an integrated radiation dose, over time. Arginine and glycine offer a similar stability, while the signals from some other amino-acids undergo changes with time, when the lifetime can be as short as 2–3 days for leucine. It was noted that after an irradiation of methionine to a dose of 5 kGy, the expected signal was entirely absent, following a 2 hour car drive from the irradiation source to the ESR lab!

It should be noted that radicals can also be induced in materials, including drugs, by mechanical processes such as grinding (Section 10), so it is important to check non-irradiated samples too, for the absence of any such signals.

7.3 Detection of irradiated foodstuffs by ESR

Although the ability of ionising radiation to kill bacteria was noted shortly after the discovery of X-rays and γ-rays, commercial food-irradiation has only been introduced quite recently (Figure 15). In 1981, a joint Food and Agriculture (FAO), International Atomic Energy Agency (IAEA), World Health Organisation (WHO) Expert committee meeting concluded that, ''the irradiation of any food commodity up to an overall dose of 10 kGy presents no toxicological hazard; hence, toxicological testing of foods so treated is no longer required''.[66] The commission of the European Communities, and the Health Authorities of many countries, concluded that these aspects had been investigated to a greater degree than for any other method of food processing; as a consequence, the radiation treatment of different foods is now legal in more than 40 countries, but

still prohibited in others. Consequently, and in order to facilitate trade in irradiated foods, regulatory authorities in all countries are seeking simple and reliable methods to determine whether foods have been treated with radiation, and to check on compliance (or otherwise) with labelling regulations[67,68].

To date, only two irradiation techniques have been used: exposure to high-energy electrons generated by a particle accelerator, or to γ-rays produced by a radioactive source, usually ^{60}Co, although ^{137}Cs has been used in some small facilities. X-rays could, in principle, also be used. The main effect of γ- and X-rays on food and other materials is Compton scattering, *i.e.* ionisation of atoms giving rise to ''secondary electrons''; these electrons, like those generated in an accelerator, cause the production of a number of other ''secondary'' electrons and ions. This cascade of secondary electrons loses energy in ionising the foodstuff molecules, with consequent production of free radicals and thereby of ''radiolytic products''. The physical, chemical and biological effects of radiation depend on the irradiation dose, which is the quantity of energy absorbed by the material, measured in units of Gray (Gy): $1\,Gy = 1\,J/kg$. The resulting beneficial effects mainly arise from damage to the DNA in viable cells from micro-organisms or living foodstuffs. For different applications, the doses usually applied are: $0.02-0.15\,kGy$, for sprout inhibition; $0.2-1\,kGy$ for disinfestation; and up to 50 kGy for sterilisation.

Some developing countries which import to Europe products that have been cleansed of infestations or bacteria by chemical fumigation are well aware that, eventually, this will be forbidden, and that irradiation may be the sole alternative, and have implemented such facilities: *e.g.* the Tangier irradiator in Morocco, which has an activity of 12,000 Ci, and is planned to be upgraded to 80,000 Ci, and in Tunisia a 100,000 Ci station has been opened. [To get some idea of their intensity, it may be recalled that 1 Curie (Ci) is equivalent to the disintegration of 1 gramme of radium, and is equal to 3.7×10^{10} Becqerals (Bq); 1 Bq corresponds to a source where one disintegration occurs per second].

ESR is only really useful when the radical species, which it detects, are stable during commercial storage of the food: this applies to the solid and dry components[66–72], in which the radicals are effectively ''matrix-isolated''. Such stable signals are formed in fish and meat bones, and also in foods containing cellulose, *e.g.* berries; crystallized sugars also yield a stable signal. The general approach may be illustrated by a study of irradiated strawberries[73], which are so treated in order to inactivate moulds which lead

otherwise to food loss. As the water content in strawberries varies from 88% to 93%, the radicals are not stable in their pulp, whereas they are stable in the achenes, which contain only 8 – 10% of water. The achenes were cut from strawberries which had been irradiated with γ-rays from a ^{137}Cs source to a dose of 1 – 3 kGy, and washed with water. In order to reduce the amount of water in the ESR sample tube, which would lead to dielectric loss, they were first air-dried on filter paper, or lyophilized. The resulting ESR spectrum contained signals from Mn^{2+} (A) and two other radicals, (C) and (D): (C) is only present in the irradiated samples, and is detected, as a shoulder, at a dose of 0.5 kGy; above 1 kGy, it was clearly present. Signal (C) is not a single line, but is the low-field member of a doublet: the high-field line is visible only at high doses and is partly obscured by the fourth line (from low-field) of the Mn^{2+} sextet. In the case of a 1 kGy dose, signal (C) remained constant after 40 days storage of the irradiated strawberries at 5°C, but became invisible after longer periods. At 2 kGy, (C) was always distinguishable; even after 40 days. Consequently, it is proposed that it may be used in the marketplace, as a test for irradiated strawberries. The line (C) is also present in other kinds of irradiated fruit, such as figs and bilberries and is particularly stable in respect of the normal commercial storage time in the case of raspberries and redcurrants, so the method may have more widespread applications[73].

8. Nitroxides

We have already noted that $R_2N\text{-}O^{\cdot}$ radicals are variously named nitroxides, nitroxyls, aminoxyls; nitroxide radicals, nitroxyl radicals, aminoxyl radicals, and of greater importance than such semantic considerations, that they are extraordinarily stable compared with most free radicals. They are, therefore, readily detected by ESR, and are frequently used as ''spin-probes'' or ''spin-labels'' (depending on whether they are merely dissolved or dispersed in the probe medium or are chemically attached to it), with which to measure molecular dynamics in many systems. They may also be used to measure the reactive metabolism of tissues, cell-cultures and other biological media, in which they are converted by either reduction or oxidation, by the fall in the intensity of their ESR signal as the reactions proceed. Some examples of these aspects are now considered.

8.1 Metabolism of nitroxides in cells and tissues

We have alluded to the fact that spin-adducts, nitroxides, produced by the trapping of radicals with nitroso or nitrone compounds, are subject to metabolism in cells and tissues. While this might be a problem in spin-trapping work, requiring the *ex vivo* treatment of samples, to re-oxidise hydroxylamines to nitroxides, so rendering them detectable to ESR, the deliberate introduction of stable nitroxides to biological media can be used as a probe of their metabolic activity and mechanism. The study of biological reactions of nitroxides has proven valuable since they respond to variables that are of considerable interest in biology, but are not readily accessed *via* other methods, *e.g.* redox metabolism, concentration of oxygen (oxygen tension), and redox agents present in tissues[11,74]. In such applications, ESR is ideal since it is quite specific for the nitroxide, even in the presence of all the other components that are, of necessity, present in the sample; tissues and dense cell suspensions are also relatively transparent to the microwave radiation used (especially at the lower, *e.g.* L-band, frequencies of *ca* 1 GHz), in contrast to optical methods, where scattering of the incident light radiation is a severe limitation[75].

8.1.1 Reduction of nitroxides in mammalian cells

There are three principal factors which determine the reactivity of nitroxides toward reduction: the nature of the ring in which the nitroxide function is contained, its lipid-solubility and its charge. The type of ring is the most important factor in the chemistry of nitroxides, conferring a relative resistance to bioreduction of pyrrolidines and pyrrolines over piperidines and oxazolidines[76]. The rates of reduction of nitroxides by cells generally parallel those measured in model systems, *e.g.* by ascorbate present in solutions[76,77] or liposome suspensions[78]; exceptions are found when either the penetration of the nitroxide into the cells is in some way limited, or the cellular metabolic efficiency is compromised. Since lipophilic nitroxides are located primarily in membrane compartments, while hydrophilic nitroxides are substantially in aqueous compartments, their relative rates of reduction reflect the efficiency of those processes occurring in each environment. Those lipophilic nitroxides most extensively studied are analogues of stearic acid with a doxyl group located at different positions along the chain[79,80]: in anoxic (low oxygen tension) cell media, the rate of reduction of the nitroxide is greatest when the function is located

near to the surface of the membrane[81,82]; in oxygen-rich samples, the overall rate of reduction is slower, and is not affected by the location of the nitroxide function. The reaction order is also different in the two cases: nitroxides near the surface show first-order kinetics with respect to the nitroxide, while those deeper in the membrane are zero-order in nitroxide concentration[11].

The observation that the rate of reduction of some nitroxides in cells is dependent on the oxygen tension has raised the possibility that it may be used in the measurement both of oxygen concentrations and redox metabolism. The rate of reduction of 5-doxyl stearate can be reduced by a factor of more than 10 in the presence of oxygen; larger than for 10-doxyl stearate, in which the nitroxide group is more deeply ''buried'' from the membrane surface[79]. In general, it appears that the role of oxygen is to modify the redox conditions of the electron-transport system in the cell.

8.1.2 Applications of the metabolism of nitroxides

It is normally assumed that the rate-limiting step for reduction of a nitroxide is its entry into the cell, since once entered, reduction is fast; therefore, the reduction of nitroxides has been used as a gauge of the transport rate across the membranes of erythrocytes[83,84]. Kinetic studies of this kind indicate that nitroxides bearing anionic groups are transported across the membranes very actively, and by at least two different mechanisms, while the transport of cations is quite slow. By measuring the reduction rates of nitroxides, following various pre-treatments of the cells such as the action of ionising radiation, the influence of such treatment on the permeability of cell membranes can be probed[83–86].

8.1.3 Differential effects of diseased vs healthy cells: a diagnostic probe of disease

It is well established that cancer cells are possessed by a different type of metabolism than are healthy cells in the corresponding tissue, and the rate of metabolism of nitroxides has been employed in the investigation of these differences. Initial such studies sought changes in the lineshape of the ESR spectra of incorporated nitroxides, anticipating differences in the fluidity of the membranes, but no conclusive results were gathered[11]. In contrast, it was observed that the reduction of nitroxides in tissue was not only efficient, but differential, so that changes in metabolism incurred by

malignant transformation might be probed. Most studies have shown an increased rate of reduction of nitroxides by cancer cells, in accord with perceived wisdom that once a cell becomes cancerous, its metabolism is switched into a higher gear[87]. It has been suggested that increased reduction of nitroxides in malignant cells might reflect the onset of this phenomenon[88]. There are, however, examples which are not consistent with this, and great variance may be found depending on the type of nitroxide (even whether it is the nitroxide-derivative of stearic acid, or of an ester of the acid); thus, membrane penetration is a key factor in locating the probe so that it may measure particular features of the cell metabolism[11].

A correlation between the ability of cells to reduce nitroxides, and the health of their tissue, more generally, might lead to such practical applications as determining human fertility, since it has been found that the ability of intact human spermatozoa to reduce nitroxides is sensitive both to the quantity and the quality of the sperm[89]. Cold shock had no effect on the rate, but inhibitors of the electron transport chain, such as rotenone, antimycin A, potassium cyanide and sodium azide, or bubbling with nitrogen or oxygen gases, changed the rate of metabolism. One can always tell that the process is indeed reduction (rather than oxidation), since the resulting hydroxylamines can be oxidised back to the ESR-detectable nitroxides by chemical oxidation[21].

8.1.4 Probe of "oxidising-species" formed in cells

Most attention regarding the metabolism of nitroxides in cells has been turned to ''reduction''; however, the oxidation of nitroxides may also prove a fruitful study. Reductions are essentially reversible, *e.g*. by bubbling with oxygen, or treatment with ferricyanide, but oxidations are not, since they convert the nitroxide to more complex products. Thus the two kinds of redox process may be evaluated from the extent of recovery of the initial nitroxide signal intensity (*i.e*. if all the metabolism were oxidation, there would be zero recovery by such further treatment, while it would be close to 100% if reduction only had occurred; the actual recovery figure gives an estimate of the contributions from both processes). There is, of course, no identification possible of the oxidising species by ESR; however, the resulting products may be examined by mass spectrometry[90], and adducts of the nitroxide with radical species, or further products derived from the oxidised nitroxide may be

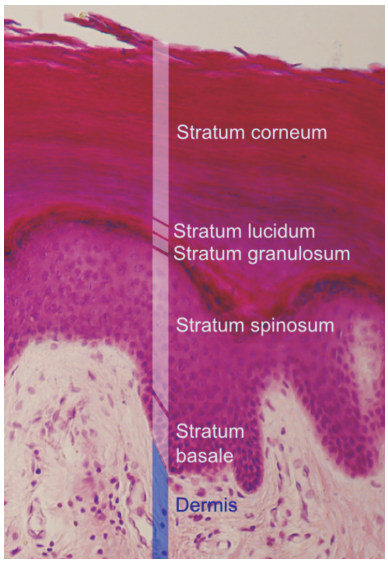

Figure 16 *Structure of the skin: the epidermal layers. Credit Mikael Haggstrom. http://upload.wikimedia.org/wikipedia/commons/e/e4/Epidermal_layers.png*

identified, so giving clues to the species involved in the oxidation process.

8.1.5 Measurement of the oxygen concentration in cells

We have seen (Section 6) that various materials containing stable free radical signals, if physically implanted in particular tissues, or introduced to their cells by phagocytosis, can provide a measure of the local oxygen concentration, since oxygen is paramagnetic and broadens their ESR spectra lines, by magnetic dipolar interactions and by Heisenberg exchange. Nitroxides may be introduced to cells for this, among other, purposes, but not all biological systems are amenable to this approach, as a calibration curve of linewidth *vs* oxygen concentration must first be made, and the concentration of nitroxide at the time of measurement be determined, which may not be possible in the system of interest. As an alternative strategy, the oxygen sensitivity of the reduction rate of a nitroxide can be used to measure the oxygen concentration; now, an accurate knowledge of the nitroxide concentration is unnecessary, and the approach is most sensitively applied under conditions of low oxygen tension (*ca* 1 μM). This has been used in studies of cell systems through the

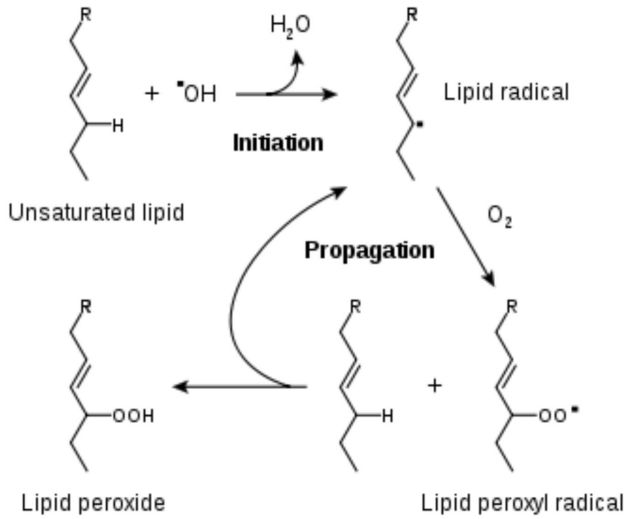

Figure 17 *The process of lipid-peroxidation. Credit Tim Vickers. http://upload.wikimedia.org/wikipedia/commons/9/9e/Lipid_peroxidation.svg*

rates of reduction of nitroxides including 5-doxyl stearate in such areas of low oxygen concentration[81,91]. The determination of low oxygen concentrations by this method has considerable potential, since various important pathological events are associated with low oxygen levels, including ischemic tissue injury and in tumours. In tumours, it is well known that the oxygen level varies within the tissue, and that very hypoxic regions may provide the determining factor for their response to therapy, since cells in hypoxic environments are relatively resistant to radiation therapy and some chemotherapeutics[92–94]. While this has been known for many years, especially in regard to radiation treatment, it has been shown more recently that hypoxia itself can induce changes in the properties of cells such that the malignancy of the tumour is increased, thus conferring an even greater importance on the ability to measure low oxygen tensions in complex, cellular environments[92–94].

8.1.6 Studies of drug-delivery into skin

The encapsulation of charged nitroxides that are capable of ready reduction into liposomes has enabled a means for monitoring liposomal transport and metabolism in biological systems. The

technique rests upon the fact that these liposome-encased nitroxides will be protected against common biological reductants like ascorbate, since neither the nitroxide nor the reductant can diffuse through the intact liposomal membrane; when the liposome is damaged by interaction with the cell or tissue, the nitroxide is set free and can then undergo reduction. One application has been to simultaneously study the spatial and temporal distribution of liposomes containing nitroxides, when they are applied to skin[95–98]. The system is considered to provide a model of the cutaneous and percutaneous delivery of drugs and other substances, such as cosmetic preparations, to the skin. Since the reductant concentration is low in the stratum corneum but is high in the keratinocytes beneath it, the rate of reduction of the nitroxides provides an excellent gauge of the delivery of liposomes through the stratum corneum (Figure 16)[99].

9. Lipid peroxidation

Lipid peroxidation (Figure 17)[100] was first studied quantitatively by Saussure, as long ago as 1820, who observed that a layer of walnut oil on water absorbed three times its own volume of air in the first 8 months; this increased to 60 times in the next 10 days, then slackened off over the next 3 months, whereupon a total absorption of 145 times its own volume of oxygen had occurred; simultaneously, the oil had become rancid and viscous. Subsequently, Berzelius proposed that such oxygen absorption might explain a variety of processes, including the fact that wool often ignited spontaneously having been lubricated with linseed oil; at that time, this was a notable scenario for catastrophe in textile mills.

In the 1940s, Farmer and others at the British Rubber Producers Association research laboratories deduced the sequence of reactions which is now understood to be the basis of lipid peroxidation: ''oxygen dependent deterioration'' or ''rancidity'' has long been recognised as a problem in the storage of fats and oils, and is even more so, now, given the favour of ''polyunsaturated'' margarines and cooking oils, and the widespread use of paints and other surface coatings, plastics and rubber, all of which can undergo oxidative degradation.

9.1 Lipids in membranes

Biological membranes[100] consist mainly of lipids and proteins; the proportion of protein increases according to the level and complexity of the membrane function. Membrane lipids are generally amphipathic molecules, which means that they contain hydrophobic regions which exclude water and also polar groups which associate with water. In animal cell membranes, the major lipid components are phospholipids, based on glycerol, but other membranes, particularly plasma membranes, contain sphingolipids along with cholesterol; the most common phospholipid in animal cell membranes is lecithin (phosphatidylcholine).

The fatty acid side-chains of membrane lipids in animal cells have unbranched carbon chains and contain even numbers of carbon atoms, mostly in the range 14–24, and the C═C double bonds are in the cis-geometry. The lipid composition of bacterial membranes depends largely on the species, but the lipid fraction is typically 10–30%. As the degree of unsaturation of a fatty-acid increases, its melting point drops, and it becomes more susceptible to oxidative degradation; however, polyunsaturated fatty-acid chains are present in many membrane phospholipids. The presence of saturated and polyunsaturated fatty-acid side-chains in many membrane lipids confers fluidity to the membrane, so that the membrane interior gains the chemical nature and viscosity of a ''light oil''; oxidative damage to polyunsaturated chains tends to reduce membrane fluidity, known to be essential to the effective functioning of biological membranes, and so their action is impaired.

9.2 The peroxidation process

In a completely peroxide-free lipid system, a carbon-centred radical is formed by H-atom abstraction from a CH_2 group of a lipid chain; $^{\bullet}OH$, widely implicated in biology, is readily capable of this [Eqn (14)]:

$$R_2CH_2 + {}^{\bullet}OH \rightarrow R_2CH^{\bullet\cdot} + H_2O \qquad (14)$$

This may be demonstrated by the radiolysis of aqueous solutions, which generates $^{\bullet}OH$; both biological membranes, fatty acids and food lipids undergo peroxidation under these conditions–the process is inhibited by agents like mannitol and formate, which are efficient $^{\bullet}OH$ radical scavengers; stimulation of lipid peroxidation in this way poses a problem in ''food irradiation'', which aims to preserve foodstuffs.

The conjugate acid of superoxide ($HO_2^{\cdot}$), which is able to cross membranes easily, is a strong contender for an ''oxygen radical'' which can initiate lipid peroxidation, although its definite role in this regard is as yet unproven.

Once the carbon centred radical is formed, it will rapidly react with molecular oxygen forming a peroxyl radical [Eqn (15)]:

$$R_2CH^{\cdot} + O_2 \rightarrow R_2CHOO^{\cdot} \quad (15)$$

The formation of lipid peroxyl radicals has been demonstrated by the ESR–''spin-trapping'' technique[10], which is described in Section 4; this approach is often used as evidence that free radical mediated processes are involved in a given system, and some recent examples of this, pertinent to lipid peroxidation, are given subsequently.

It might be envisaged that peroxyl radical formation occurs competitively with other processes, such as radical combination or attack on other membrane components; the effective oxygen concentration might determine the relative effectiveness of these pathways, as may the ''anchoring'' of the carbon radicals within the membrane structure.

The peroxyl radicals then enter the propagation phase, in which they abstract a hydrogen atom from another lipid chain, forming a lipid hydroperoxide [Eqn (16)]:

$$ROO^{\cdot} + R_2CH_2 \rightarrow ROOH + R_2CH^{\cdot} \quad (16)$$

The ''new'' radical can react with another O_2 molecule, and the entire process be repeated, so constituting a chain-reaction. Since the initial H-atom abstraction can occur at different points on the carbon chain, the products of lipid peroxidation are often formed as complex mixtures: *e.g.* the peroxidation of arachidonic acid gives certainly 6 different hydroperoxides along with cyclic peroxides and other products.

9.3 Protection against lipid peroxidation

Unsaturated fatty-acids, dispersed in organic solvents, or with detergents in aqueous solution, are readily peroxidised; phospholipids, similarly, are more rapidly peroxidised in simple micellar structures than in lipid bilayers. Ingold has proposed[101] that this is due to the relatively more polar character of lipid peroxyls than unreacted hydrocarbon chains, which thus tend to avoid the weakly polar membrane interior, moving toward the bilayer surface, so reducing the initiation efficiency.

The presence of cholesterol also exerts an influence on the peroxidation sensitivity of surface membranes, probably by a combination of radical scavenging and modification of the internal structure of the membrane.

The susceptibility of a membrane to oxidative damage is also modified significantly by the presence of positively charged ions, which probably bind to the negatively charged head-groups of the phospholipid: this is manifested either by an increase or decrease in the rate of peroxidation. For instance, a number of metal ions, *e.g.* Ca^{2+}, Co^{2+}, Cd^{2+}, Al^{3+}, Hg^{2+}, Pb^{2+}, have been shown to alter the rate of peroxidation of liposomes, erythrocytes and microsomal membranes: in general, peroxidation induced by the addition of iron ions is stimulated by their presence; the inhibiting influence of Zn^{2+}, Mn^{2+} or polyamines, found in certain cases, may be due to their ability to displace iron ions from phospholipid binding sites.

9.4 Antioxidants

Since lipid peroxidation is a ''bad'' thing, particularly in the biological context, where it destroys the essential integrity of membranes and so compromises their biological function, including the compartmentalisation effect so fundamental to the cellular system, ways of avoiding, or at least ameliorating, the process are of concern. We hear much, currently, of the role of antioxidants in the diet, which are thought to protect against the development of a variety of diseases, and even the process of ageing itself.

Antioxidants are generally regarded as ''radical scavengers'' (Section 4.5): intercepting free radicals before they can attack sensitive cellular components, including the membranes themselves.

In biological membranes, vitamin E is a highly effective anti-oxidant, thought to act by chain-breaking, since it is a phenol [Eqn (17)]:

$$\mathrm{Vit-E-OH + ROO^{\cdot} \rightarrow Vit-E-O^{\cdot} + ROOH} \qquad (17)$$

It has been further argued, that vitamin E also modifies the structure of membranes, since a protective effect is found even when vitamin E acetate is used (*i.e.* the reactive phenolic H-atom has been removed)[102].

9.5 Lipid peroxyl radicals

9.5.1 Direct studies by ESR

As stated earlier, peroxyl radicals are involved in the destruction of cell membranes, and in the rancidification of fats and oils, by lipid peroxidation, and there is the aim to prevent, or at least to ameliorate the related undesired effects, by means of deactivating these radicals which drive them. We have stressed that one solution is to administer ''antioxidants'', some being phenolic, which can readily scavenge reactive radicals including peroxyl radicals. Hereby motivated, Sevilla and his co-workers have used ESR in order to elucidate the mechanisms of reactions between carbon centred radicals derived from lipids and phenolic antioxidants (*tert*-butylhydroquinone TBHQ, *n*-propyl gallate PG, butylated hydroxyanisole BHA, butylated hydroxytoluene BHT and vitamin E), using the lipid as a matrix at low temperatures[103]: in all cases, the carbon centred radicals were found to react at 135 K with molecular oxygen, forming peroxyl radicals. At 170 K, the peroxyl radicals were found to react with the added antioxidants, forming the corresponding phenoxyl radicals: those derived from tributyrin were found to decrease in their rate of reaction in the order BHT > TBHQ > E > PG > BHA, while those derived from triolein and trilinolein decrease in the order BHT > E > BHA > TBHQ; these differences are accounted for in terms of the way the antioxidants are dispersed in the different matrices. The fraction of unsaturated lipid peroxyl radicals which abstract from the antioxidant is lower than that in saturated lipids, and in the case of tributyrin the initial carbon centred radicals can abstract directly from the antioxidant, while those more stable, conjugated, radicals derived from unsaturated lipids do so only to a negligible extent; the decay of all five antioxidant phenoxyl radicals in tributyrin follows second order kinetics with an apparently common activation energy of 23 kcal/mol. The same group previously determined the reactivity of radicals formed from cholesterol and its analogues by γ-irradiation[104]. In oxygen-free samples of cholesterol itself are produced a tertiary side-chain radical and an allylic radical – the structure of the latter is confirmed by experiments using two cholesterol analogues, namely 7-hydroxycholesterol and the selectively deuterated 7-deutero-7-hydroxycholesterol, both of which produce the allylic radical after radiolysis by loss of the hydroxyl group. When oxygen is present in the samples, evidence is provided for the formation of two distinct peroxyl radicals, and these are

suggested to possess differing reactivities resulting from their differential motional freedom; it is further suggested that the products detected following radiation-induced autoxidation at or close to ambient temperature are consistent with the differing reactivities of these intermediary peroxyl radicals.

The autoxidation phenomena has also been explored for the lipids tributyrin, triarachidin, triolein, triliolein, trilinolenin and linolenic acid[105]. It was found that the *unsaturated* lipids generally contained sufficient hydroperoxides that their direct U.V. photolysis as neat samples at 77 K resulted in intense ESR signals; in contrast, it was necessary either to add *tert*-butyl hydroperoxide to the samples of *saturated* lipids prior to photolysis, or instead to use γ-irradiation of the pure material: the latter being found to give a more even distribution of radicals in the sample. Diffusion of molecular oxygen was found to occur in each case at a particular temperature, which is characteristic of the particular lipid, when it reacts with those carbon centred radicals produced initially, and forms the peroxyl radicals. Most interestingly, for unsaturated lipids the peroxyl radicals were found to decay with further annealing with the concomitant production of the lipid allylic or pentadienyl radicals, respectively, depending on the number of double bonds in the chains: we see, then, the essential free radical chemistry involved in the peroxidation process – a hydrogen atom is abstracted from a weak C—H bond, the resulting stabilised radical then adds molecular oxygen to form a peroxyl radical, which then abstracts a weakly bound hydrogen atom (as in Figure 17). In experiments with linolenic acid, subsequent introduction of oxygen resulted in the formation of further peroxyl radicals at low temperatures but the signal from the pentadienyl radical was found to prevail at higher temperatures; an explanation is proposed in terms of the relative rates of oxygen migration and hydrogen atom abstraction processes.

An investigation of the kinetics of the autoxidation of triglycerides was published 3 years later, again using ESR[106]. It was found that, following the initial production of carbon centred radicals the following *distinct reaction stages* then occur: formation of peroxyl radicals by addition of O_2 molecules, and so the depletion of the oxygen content of the sample; conversion of the lipid peroxyl radicals into allylic or pentadienylic radicals, by hydrogen atom abstraction; finally, combination of these carbon centred radicals. From the kinetics of these stages it is concluded that the peroxidation step is controlled by O_2 diffusion which has an apparent activation energy of 24 kJ/mol in unsaturated lipids. The subsequent H-atom abstraction step (autoxidation cycle) depends on the

lipid structure, and partly on the relative C—H bond strength for the atom being abstracted, since the activation energies are 9 ± 2, 34 ± 8, 88 ± 11 kJ/mol, for trilinolenin, trilinolein and triolein, yielding radicals conjugated presumably with two C═C double bonds in the former two cases, but with only one C═C bond in the latter; the cause of the difference in activation energy between trilinolenin and trilinolein is not clear. In the final stage, these carbon centred radicals combine at temperatures approaching the softening point of the particular lipid matrix, with a common activation energy of *ca* 40 kJ/mol. For saturated lipids, the peroxyl radical signal decays with second order kinetics, indicating a bimolecular radical combination mechanism. In contrast, the unsaturated lipid peroxyl decay, which is unimolecular, can be explained on the basis that the strength of the ROO—H bond is less than that of a C—H bond in a *saturated* molecule thus preventing its mode of decay by H-atom abstraction.

9.6 Some recent examples of spin-trapping in lipid peroxidation

We have discussed generally oxidative damage to lipids, above, in which an initial carbon centred radical is formed by H-atom abstraction from an ''allylic'' CH_2 group; however, a recent study[107] has provided some indication that radical attack on the glyceryl moiety of a phospholipid, producing the corresponding 2-glyceryl radical might precipitate lipid damage *via* rapid beta-cleavage of the adjacent C—O bond, releasing an acyl radical. Moreover, the rate of cleavage is greater in non-polar solvents, at least in model systems, so it may be particularly effective in membranes.

In addition to the ubiquitous implication of the $^{\bullet}OH$ radical in all manner of disease states, ''peroxynitrite'' follows from the almost equally ubiquitous ''nitric oxide'' (NO), which can form peroxynitrite/peroxynitrous acid by reaction with superoxide [Eqn (18)]:

$$NO + O_2^{-\cdot} \rightarrow {}^{-}OONO/HOONO \qquad (18)$$

Peroxynitrite may be considered as a toxic form of NO, and is formed either inadvertently or deliberately in the cellular defense mechanism. Being strongly oxidising, it is believed capable of initiating lipid peroxidation, and is the subject of many investigations.

9.6.1 Thiyl radicals in lipid peroxidation

In one study, the decomposition of peroxynitrite (HOONO) in the presence of the spin-trap 5,5-dimethyl-1-pyrroline-N-oxide (DMPO) generated 5,5-dimethyl-2-pyrrolidone-1-oxyl, without generation of the $^{\cdot}$OH adduct of DMPO; the peroxynitrite decomposition was enhanced by formate but no formate derived radicals were generated. Glutathione, cysteine, penicillamine and ascorbate reacted with peroxynitrite to generate the corresponding thiyl and ascorbyl radicals. The results show that the decomposition of peroxynitrite does not generate significant amounts of $^{\cdot}$OH radicals and that single-electron reduction of peroxynitrite by ascorbate may be one of the important detoxification pathways[108]. Of course, as in all detoxification mechanisms which produce secondary radicals, the subsequent fate of these radicals is a matter of concern: *e.g.* for thiyl radicals, which are highly reactive, especially in non-polar media[9]. Oxidation of thiols, present in cells to defend against reactive radicals, often results in the formation of thiyl radicals, which although generally undetectable in solution by ESR, directly[109] may be spin-trapped. A novel phosphorylated spin-trap, 5-diethoxyphosphoryl-5-methyl-1-pyrroline-N-oxide, which may be considered an analogue of DMPO, has been used to investigate the reactions of sulfur centred radicals produced by the oxidation of thiols with peroxynitrite[110]. In all cases, the predominant species trapped is the corresponding thiyl radical, from glutathione and N-acetyl-DL-penicillamine, but the sulfite radical anion from sulfite ions. All these radicals react with ammonium formate to form the $CO_2^{-\cdot}$ radical anion. It is concluded that the direct reaction of peroxynitrite with thiols and with sulfite forms thiyl radicals and the sulfite radical anion by a mechanism independent of $^{\cdot}$OH radicals; pathological implications of thiyl radical formation, and subsequent oxyradical mediated chain reactions, are discussed. It is suggested that oxygen activation by thiyl radicals formed during peroxynitrite mediated oxidation of glutathione (GSH) may limit its effectiveness against peroxynitrite mediated toxicity in cells.

In a re-examination of the formation and reactions of radicals formed by the peroxynitrite mediated oxidation of thiols and sodium bisulfite, it was found that thiyl radicals were indeed formed from GSH, L-cysteine and N-acetyl-D,L-penicillamine, but the sulfite radical anion was formed from bisulfite, as detected by spin-trapping. Additionally the formation of the OH—DMPO adduct was completely inhibited by low M.W. superoxide dismutase (SOD) mimics. This suggests that the

OH—DMPO adduct originates from the decay of the superoxide radical adduct of DMPO. In the presence of these SOD mimics, the DMPO-sulfur radical adducts were more persistent, implying that superoxide is partly responsible for their decay. Again, the origin of these sulfur radicals by an $^{\cdot}OH$ radical independent mechanism is concluded[111].

Using a low-frequency (1.1 GHz; L-band) ESR spectrometer, the hemoglobin thiyl radical was detected in living rats. The radical was spin-trapped using DMPO, in blood samples, following the intragastric administration of phenylhydrazine. Pretreatment of the rats with ascorbate and diethylmalonate decreased the signal intensity; incubation of diethylmalonate with rat blood containing preformed thiyl radical adduct showed no effect on the signal, while incubation with ascorbate caused a reduction in its intensity, so providing direct evidence that the hemoglobin thiyl radical is formed *in vivo* and may be studied as such, free from artifacts that can occur when using *ex vivo* methods[112].

9.6.2 Haloalkyl radical initiated peroxidation

Following immediately from the previous section on thiyl radicals is a study of the role of thiyl radicals in lipid peroxidation by CCl_4 derived radicals[113]. Elevation of cellular calcium levels has been shown to occur after exposure to hepatotoxins such as CCl_4, and has been associated with inhibition of the Ca^{2+}, Mg^{2+}-ATPase which pumps calcium into the endoplastic reticulum. Elevated Ca^{2+} may also result from activation of calcium releasing channels. In the presence of NADPH, CCl_4 produced a concentration-dependent release of calcium from liver microsomes, but after a time lag. The lag period was shorter with microsomes from pyrazole treated rats in which the enzyme CYP2E1 (a cytochrome P450) is induced. The calcium release process appears to be very sensitive to activation by CCl_4, and it is indicated that CCl_4 metabolism is required for the activation of its release. Production of CCl_3 was shown by spin-trapping experiments, which further demonstrated that calcium release was prevented by the presence of spin-traps, confirming that CCl_3 and possibly other reactive radicals are indeed required. It is notable that lipid peroxidation was not observed at the levels of CCl_4 used. CCl_4 induced calcium release could be partly reversed by lipophilic thiols such as mercaptoethanol or cysteamine, whereas GSH was ineffective; so the activity is present exclusively in the membrane[113].

There is concern over the toxic – especially carcinogenic – effects of chromium compounds. One paper[114] reports the formation of $CCl_3^{\cdot}$ radicals in the livers of mice which had been administered Cr(III); the lipid peroxidation in liver microsomes induced *in vitro* by CCl_4 in the presence of NADPH was decreased by the preadministration of Cr(III) to the mice. The activity of NADPH-cytochrome c reductase, which presumably catalyses the formation of $CCl_3^{\cdot}$ from CCl_4 in liver microsomes, was depressed by Cr(III) administration and remained lower for at least 2 hours after dosing with CCl_4 than the control group. Spin-trapping in the liver homogenate demonstrated that $CCl_3^{\cdot}$ production was reduced by Cr(III) preadministration in a manner similar to DL-alpha-tocopherol. It is believed that Cr(III) actually scavenges $CCl_3^{\cdot}$ radicals in the liver cells. However, another group[115] reported a study of the protective role of Cr(III) and also Zn(II) and metallothionein against CCl_4 toxicity *in vivo*. Their conclusion is that there is no difference in either the amount or in the rate of formation of $CCl_3^{\cdot}$ metabolites in the presence of these agents compared with the control. Another study used the formation of $CCl_3^{\cdot}$ spin-adducts as a measure of the conversion of CCl_4 to $CCl_3^{\cdot}$ radicals *in vivo*; this primary bioactivation step was found to occur at similar rates in female rats aged 5, 14 and 28 months, and so the attenuation of CCl_4 induced hepatotoxicity is not explained on the basis of decreased bioactivation to reactive species[116].

9.6.3 Studies of lipid peroxides

As discussed earlier, a crucial event in lipid peroxidation is abstraction of a hydrogen atom by a lipid peroxyl radical, forming a hydroperoxide: this is a propagation step since a carbon centred radical is also produced, which can add dioxygen to form another peroxyl radical. Since the products of lipid peroxidation arise partly from subsequent reactions of lipid hydroperoxides, an incentive is provided for their study, as in the following examples.

Cr(IV) is known to mediate free radical production from thiols, and in a study of cysteine and penicillamine, with hydrogen peroxide and model lipid peroxides, using spin-trapping, thiyl radicals were detected[117]. With cysteine, the radical became detectable at a relative cysteine:Cr(IV) concentration of *ca* 5, reached its highest level at *ca* 30 and thereafter declined; similar results were obtained with penicillamine. Incubation of Cr(IV), cysteine or penicillamine and H_2O_2 led to $^{\cdot}OH$ radical generation,

as was verified by quantitative competition experiments using ethanol. The mechanism is considered to be a Cr(IV)-mediated Fenton type reaction. When model lipid hydroperoxides such as tert-butyl hydroperoxide and cumene hydroperoxide were used instead of H_2O_2, hydroperoxide radicals were produced. It is suggested that since thiols such as cysteine exist in cells at relatively high concentrations, Cr(IV)-mediated free radical generation in the presence of thiols may participate in the mechanisms of Cr(IV)-induced toxicity and carcinogenesis.

On the toxicity of thiols, an independent study has shown that thiyl radicals generated from cysteine and glutathione by nitrogen dioxide enhance the lipid peroxidation of liposome composed of 1-palmitoyl-2-arachidonylphosphatidylcholine. ESR spin-trapping using DMPO confirms the presence of thiyl radicals, while additional analysis shows the effective induction of both lipid peroxidation and DNA strand breaks[118].

The relative toxicities of methyl linoleate-9,10-ozonide (MLO) and cumene hydroperoxide (CumOOH) have been compared[119]. Both agents caused a dose-dependent decrease in the phagocytosing activity of alveolar macrophages isolated from rat lungs; MLO was found to be three times more toxic than CumOOH. Supplementation of the macrophages with vitamin C caused a decrease in their sensitivity towards MLO but an increase in their sensitivity towards CumOOH, suggesting that different mechanisms underlie their toxic action. This was supported by data obtained on GSH and vitamin E depletion: in both cases, depletion of the antioxidant was more extensive on exposure to CumOOH; additionally, following GSH depletion, the sensitivity of the macrophages towards CumOOH was more increased than towards MLO. Further, MLO was unable to enhance peroxide formation from methyl linoleate, whereas CumOOH initiated its peroxidation. The results of ESR spin-trap experiments further support that MLO-induced toxicity is independent of lipid peroxidation.

From all of this, it is concluded that both mechanisms known to be of importance in peroxide-induced cell toxicity, *i.e.* depletion of cellular GSH levels and/or lipid peroxidation are not the main processes leading to MLO toxicity *in vivo*.

Endothelial cells have been shown to generate primary oxygen-centred radicals[120] ($^{\cdot}OH$, $O_2^{-\cdot}$) during post-anoxic reoxygenation, but little evidence is available concerning subsequent initiation of lipid peroxidative injury. ESR spin-trapping, using phenyl-tert-butyl nitrone (PBN), was employed to monitor lipid derived free radicals formed by cultured bovine aortic endothelial cell suspensions

subjected to anoxia (N_2 gas for 45 minutes) followed by reoxygenation (95% O_2, 5% CO_2 for 15 minutes). In some experiments, SOD (10 μg/mL) was introduced immediately prior to reoxygenation to assess the effects of this primary free radical scavenger on lipid radical production. At various times, aliquots were removed and PBN was introduced to either the cell suspension or to the corresponding cell-free filtrate, prior to extraction with toluene and ESR analysis. A lipid derived alkoxyl radical adduct of PBN was detected during reoxygenation using both procedures, with maximal production at 4–5 minutes followed by a second maximum at 10 minutes; SOD effectively reduced the RO. production. HPLC analysis of hydroperoxide production showed comparable maxima at 4–5 minutes and 10 minutes implicating the $RO^{\cdot}$ radicals in the peroxidation mechanism.

The mechanism of free radical production from hydroperoxides by cytochrome c has been investigated[121]. When *tert*-butyl hydroperoxide and cumene hydroperoxide were treated with the enzyme in the presence of DMPO, the presence of methyl, peroxyl and alkoxyl radicals was demonstrated. From detailed analysis of the relative concentrations of these species, it was concluded that the alkoxyl radical was that initially produced from the hydroperoxide, presumably by homolytic cleavage of the O—O bond by ferric cytochrome c; this contrasts a previous study which proposed a heterolytic mechanism for the reaction of cytochrome c with hydroperoxides. Methyl radicals were produced by beta-scission of the alkoxyl radicals, while the peroxyl radicals are shown to be secondary products arising from the reaction of dioxygen with methyl radicals ($MeOO^{\cdot}$). In separate experiments, visible absorption spectroscopy revealed that the heme centre of the cytochrome c was destroyed during the reaction; both the heme destruction and the production of radical adducts were inhibited by addition of cyanide, presumably by the formation of a cyanoheme complex.

From the same laboratory comes another study, this time of the action of cytochrome P450 on cumene hydroperoxide[122]. Cumene hydroperoxide derived peroxyl, alkoxyl and carbon centred radicals were formed and spin-trapped during the course of the reaction; by means of 2-methyl-2-nitrosopropane as the spin-trap, the carbon centred radicals were identified as methyl, hydroxymethyl and a secondary carbon centred radical ($R_2CH^{\cdot}$). The reaction did not require NADPH-cytochrome P450 reductase or NADPH, and the proposed mechanism is as above for cytochrome c.

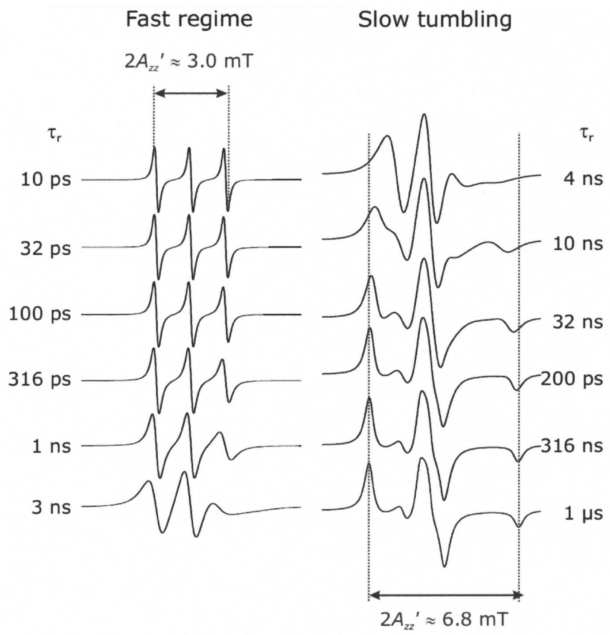

Figure 18 *Effect of reorientation rate on the ESR spectrum of a nitroxide spin-probe. As the medium becomes more viscous the lines (especially the high field line) first broaden and then a more complex spectral pattern arises. Simulations performed with Easyspin: Stoll, S. and Schweiger, A. (2006)* J. Magn. Reson., **178**, *42.*
http://www.epr.ethz.ch/news/Bordignon_tutorial_Nitroxide_spectrum_analysis.pdf
Reproduced with permission.

The reaction of cytochrome P450 with linoleic acid hydroperoxide was also studied and compared with chemical systems where $Fe(II)SO_4$ or $Fe(III)Cl_3$ was substituted for cytochrome P450[123]. In the P450 system, DMPO adducts of $^{\cdot}OH$, $O_2^{-\cdot}$, peroxyl, methyl and acyl radicals were detected; the same radicals were found in the $Fe(II)SO_4$ system, but only the $^{\cdot}OH$ and carbon centred radical adducts were detected using $Fe(III)Cl_3$. It is proposed that polyunsaturated fatty acid hydroperoxides are initially reduced to form alkoxyl radicals, which then undergo intramolecular rearrangement to form epoxyalkyl radicals: the epoxyalkyl radical then reacts with dioxygen to form a peroxyl radical which decomposes with the elimination of $O_2^{-\cdot}$.

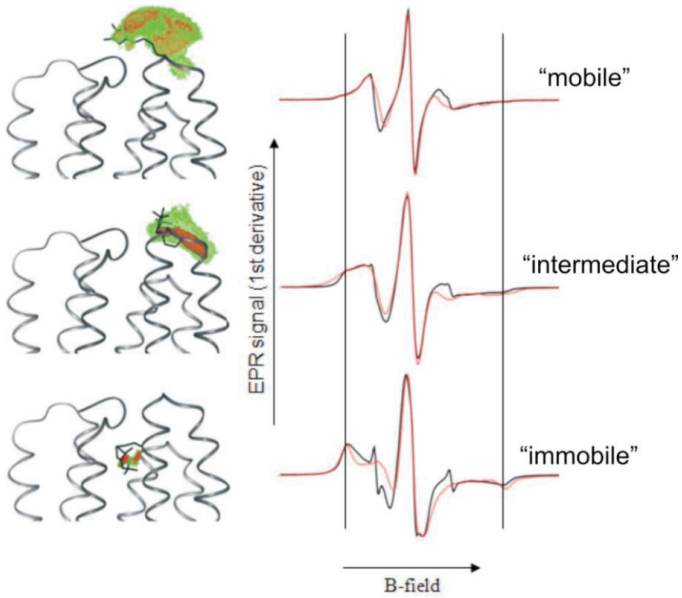

Figure 19 *Nitroxide (spin-lable) bound to a protein: influence of molecular motion on ESR spectrum. Continuous wave (CW) spectra measured at 293 K. From Beier, C. and Steinhoff, H.J. (2006)* Biophys. J.*,* **91***, 2647 http://www.epr.ethz.ch/news/Bordignon_tutorial_Nitroxide_spectrum_analysis.pdf Reproduced with permission.*

10. Spin labelling

10.1 Background to method

Essentially, this technique[124] involves the incorporation of a stable radical, usually a nitroxide, into a medium as a probe of molecular mobility, and rests upon the averaging of anisotropic g- and hyperfine tensors, as is illustrated in Figure 18. At one extreme is the limit of fast motion, where the molecules are tumbling very rapidly and the anisotropies of the tensors are completely averaged, and the spectrum shows 3 lines of equal intensity, spaced by the isotropic ^{14}N coupling constant and centred on the isotropic g-factor. The intermediate situation is called the region of ''intermediate motion'' where the anisotropies are not completely averaged, but their presence results in an asymmetric broadening of the lines, as shown, being greatest for the high field line. By a detailed analysis of these lineshapes, it is possible to derive the rate of motion of the probe and thus the local degree of motion of its environment.

As described above, the onset of such rotational motion causes the three lines to appear with differing intensities and widths. The EPR spectrum is insensitive to molecular motion faster than *ca* 10^{-12} s, but that occurring on a timescale of *ca* $10^{-9} < \tau_c < 10^{-11}$ s, results in line-broadening. From the relative intensities (heights) of the lines associated with the $+1,0,-1$ nuclear spin states, V_{+1}, V_0, V_{-1}, the width of the central line ΔH_o, and the Eqns (19) and (20), values for the rotational correlation time τ_c of the radical can be estimated. When the reorientational motion is isotropic, Eqns (19) and (20) should give the same answer, but their estimates will differ when there is anisotropy present, *i.e.* the probe tumbles more rapidly about one axis than others.

$$\tau_c = 6.6 \times 10^{-10} \Delta H_o [(V_0/V_{-1})^{\frac{1}{2}} + (V_0/V_{+1})^{\frac{1}{2}} - 2] \qquad (19)$$

$$\tau_c = 6.6 \times 10^{-10} \Delta H_o [(V_0/V_{+1})^{\frac{1}{2}} - (V_0/V_{-1})^{\frac{1}{2}}] \qquad (20)$$

The nitroxide may simply be dissolved in an appropriate medium, to probe its viscosity, since the correlation time is directly related to the viscosity η according to Eqn (21); it is also clear that as molecules become larger (r is their radius), or if the viscosity of the medium (η) increases, they move more slowly, in accord with common sense.

$$\tau_c = 4\pi\eta r^3/3kT \qquad (21)$$

In studies of proteins, or of membranes, the nitroxide is chemically attached to a molecule whose motion it is desired to study; in this case, the motion of the nitroxide (spin-label) reflects the motion of the fragment to which it is attached (Figure 19). Particularly in this kind of situation, the motion is anisotropic, and complex theoretical models must be applied to analyse the spectra, leading to details of the type of motion and its rate about each axis. At sufficiently high concentrations, nitroxides can be used to probe lateral (translational) diffusion, on the basis of the line-broadening which results from the interactions between the unpaired electrons in two radicals which have diffused together.

10.2 Spin-labelling studies of membranes

The literature on spin-labelling studies of membranes is enormous and covers many diverse aspects of membrane function and biochemistry; but we hope to have illustrated some major recent advances in the understanding of membrane properties using spin-

labelling techniques. As an introduction to this field, there is an excellent review[125] of magnetic resonance studies of membranes, which includes both spin-labelling and NMR work. Membranes provide highly anisotropic environments, due to the regular arrangement of their constituent molecules, each with its own anisotropic properties. The molecular packing in lipid membranes varies from the tight orthorhombic lattice of the L_c phase, to the loose and hexagonal packing of molecules in the liquid crystalline L_α phase. Micro-viscosity differences of many orders of magnitude between these phases (which is almost like a solid crystal in L_c, but similar to a liquid in L_α) confer similarly large differences in the motional rates for lipid molecules. ESR methods are of particular aid in studying membrane molecular motion, since they are sensitive over the relevant millisecond to nanosecond timescales involved, which are also the timescales of numerous biological events. Almost certainly there is close connection between membrane function and molecular motion. There are three main kinds of molecular motion that may be determined by ESR for lipids, which are described as: angular rotation, lateral diffusion and trans-bilayer movement (also termed flip-flop). This is an extremely important field, and hence is given mention to in the present review; however, as there have, accordingly, been some excellent reviews written on the subject, in general, I invite the reader to these for more complete details[126,127].

10.2.1 Selected examples

A model previously developed for describing the dynamics of flexible alkyl chains has been adapted to the analysis of spin-label spectra obtained from an oriented phospholipid membrane: in this model, rotation around each C—C bond of the labelled alkyl chain is characterized by two inequivalent minima, with one end of the chain fixed to mimic the phospholipid headgroup, and with the dynamic effects of the nitroxide label included explicitly. This model is integrated with that for the overall rotation of the phospholipid in the mean orientational potential of the aligned membrane, and it is incorporated into the stochastic Liouville equation which describes the ESR lineshape in the presence of these dynamic processes. The analysis is simplified by introducing the fact that the relatively rapid internal modes of motion can be treated by motional narrowing theory and a time scale separation can be made with respect to the much slower overall motions of the phospholipid. A series of ESR spectra from the spin-label 16-PC in

the lipid dimyristoylphosphatidylcholine were obtained in the range of temperature 35–65°C in the L-alpha phase for various orientations of the normal to the bilayer plane relative to the magnetic field. Very good agreement with experiment is obtained from this model by using least squares fitting[128].

Another paper by this group reports[129] a study of lipid-gramicidin interactions using 2-dimensional Fourier-transform ESR. It is shown that 2D-FT-ESR spectra provide substantially enhanced spectral resolution to changes in the dynamics and ordering of the bulk lipids – as compared with c.w. ESR – that result from addition of gramicidin to membrane vesicles of phosphatidylcholine in excess water containing 16-PC as the lipid spin-label. Both the rotational and translational diffusion rates of the bulk lipid are substantially decreased by addition of gramicidin (GA), whereas the ordering is only slightly increased, for a 1 : 5 ratio of GA to lipid.

No significant evidence is found in the 2D-FT-ESR spectra for a second immobilised component, which is seen in c.w.-ESR measurements, and simulations of the FT spectra suggest that this component, usually ascribed to ''immobilized'' lipid is inconsistent with its being characterized by increased ordering, but is more consistent with a component with a significantly reduced diffusion rate. This is because the 2D-FT-ESR spectra exhibit a selectivity, favouring components with longer homogeneous transverse relaxation times.

2D-FT and c.w. ESR spectra at X-band frequencies were recorded over a broad range of temperatures covering the solid and melt states of a liquid crystalline polymer. The c.w. spectra were analysed using conventional motional models. The nematic phase was macroscopically aligned in the magnetic field, whereas the solid state showed microscopic order but macroscopic disorder; an end-label on the polymer showed smaller ordering and larger reorientational rates than that of the cholestane spin-probe dissolved in the same polymer, since the former cam reorient by local internal chain modes. It was demonstrated that the 2D-FT-ESR experiments provide greatly enhanced resolution to the order and dynamics of the end-label, especially when performed as 2D-ELDOR (electron-electron double resonance) experiments as a function of the mixing time. Instead of the conventional model of Brownian reorientation, a model of a slowly relaxing local structure which enables differentiation between the local internal modes experienced by the end-label and the collective reorganization of the polymer molecules around the end-label, yielded much improved fits to the experiments in the nematic phase[130].

In the functioning of a biological membrane, lipid-protein interactions play a major role. It has been found that the stoichiometries of lipid-protein interactions, obtained from spin-label ESR experiments with integral membrane proteins, deviate from values predicted from simple geometric models for the intramembranous parameter that are based on the predicted numbers of transmembrane helices: these deviations provide evidence for oligomerization of the protein in the membrane and/or the existence of more complex arrangements of the transmembrane segments[131].

The specific binding of hen egg white avidin to phosphatidylcholine lipid membranes containing spin-labelled N-biotinylphosphatidyethanolamines was investigated by ESR[132]. Spin-labelled derivatives were prepared with the nitroxide group at position C-5, C-8, C-10, C-12 or C-14 of the lipid chain, and binding of avidin caused a strong and selective restriction of lipid mobility at all positions of labelling. Overall, the results indicate that the biotinylphosphatidylethanolamines are partially withdrawn from the membrane, with a vertical displacement of $7-8$ Å, on complexation with avidin.

Conventional ESR of spin-labelled lipids and saturation-transfer ESR of spin-labelled proteins are used to study lipid-protein interactions and the mobility of integral proteins, respectively, both in biological membranes and in reconstituted lipid-protein systems. Conventional ESR reveal 2 spin-labelled lipid populations, the mobility of one being hindered by direct interaction with the integral membrane proteins[133]. The proportion of the latter component increases with increasing protein content and with increasing selectivity of the lipid species for the protein. Lipid exchange rates at the protein interface obtained by spectral simulation are found to be consistent with fast-exchange found by 2H-NMR on similar systems and to reflect the lipid selectivity observed by ESR. Protein-reactive covalent labels were used to study the rotational diffusion and aggregation states of membrane proteins *via* saturation-transfer ESR. The integral protein rotation is uniaxial and the anisotropic motion is analysed to obtain the principal component of the diffusion tensor: this is sensitive to the cross-sectional dimensions of the protein in the membrane, and hence to its state of assembly. A variety of novel experiments based on the power saturation properties of the spin-labelled components were also used to determine lipid exchange rate, protein translational diffusion rates, and the location and penetration of proteins in membranes.

Finally, we mention the use of very-high frequency (94.3 GHz) ESR in a determination of the partitioning and dynamics of 2,2,6,6-

tetramethyl-1-piperidinoxyl nitroxide radicals in large unilamellar liposomes. The nitroxide was completely resolved in both lipid and aqueous phases on account of the large resolution of the differing isotropic g-factors in the 2 media[134].

11. Free radical assay technique (FRAT)[135]

Most notably, this method was used to detect the abuse of morphine by American soldiers during the Vietnam War (1955–1975), one of the world's most infamous proxy-conflicts in the struggle between the ideologies of Western Capitalism and Communism. The technique involved is one of spin-labelling, but in which the interpretation of the results is quite simple and does not require detailed spectral analysis. One merely needs to recognize the difference between the ''sharp'' three-line spectrum of a rapidly rotating (''free'') spin-label (nitroxide radical) and the signal from an ''immobilized'' spin-label. The drug to be detected is prepared with a spin-label attached to it and premixed in solution with a known concentration of an antibody to the drug. The spin-labelled drug is firmly bound by the antibody, which being a large molecule results in a broad ''immobilized'' ESR spectrum. By suitable adjustment of the concentrations of both antibody and labelled drug, all of the drug ends up bound by the antibody, and thus there is no ''free'' sharp three-line signal present. For the immunoassay, a sample suspected to contain the drug is added to the solution of the antibody and the spin-labelled drug. Since some of the bound spin-labelled drug molecules are exchanged by the unlabelled drug molecules, a sharp three-line spectrum from ''free'' spin-labelled drug molecules is observed, and it is merely the presence of this that confirms the presenece of the drug of abuse. The method was first used to detect morphine, and the measurement is very rapid, taking just one minute to do. Morphine derivatives such as codeine and ethylmorphine (Dionin) and a morphine metabolite, morphine glucoronide could also be detected using the same antibody. However, morphine replacements (as are given to addicts to control the cravings of their addiction) such as methadone and propoxyphene (Darvon) and unrelated drugs like barbiturates and amphetamines are not recognized by the antibody. The FRAT method has been adapted to provide assays for metabolites of cocaine, barbiturates, amphetamine and methadone, although the details are not to be found in the open literature for reasons of commercial secrecy.

12. ESR for cancer diagnosis and monitoring[136]

Tumour cells release a variety of bioactive proteins and petide fragments into the blood which can bind to serum albumin, leading to structural and functional modifications. The proteins are reflective of diverse tissue and cellular origins and may thus give important disease-related information. They may also indicate the physiological state of the tumour and reveal the effects that the tumour has on the organism itself. Albumin has a very high affinity for stearic acid and hence the spin-probe, 16-doxylstearic acid was used to investigate the binding variables as monitored by ESR. Blood samples were taken from a population of healthy volunteers and blood donors ($n = 349$), patients with a wide variety of hematologic and nonhematologic malignancy ($n = 135$), and patients with chronic diseases such as gastrointenstinal and pulmonary disease, diabetes and cirrhosis ($n = 91$). By adding differing amounts of 16-doxyl-stearic acid in ethanol to 50 μl of serum from each patient, three aliquots were produced that differed in hydrophobicity and spin-probe concentration and which were incubated for 10 minutes at 37°C prior to measurement by ESR. Composite ESR spectra were obtained that could be analysed in terms of four components: (i) 16-doxyl-stearic acid bound to high-affinity fatty-acid binding site on albumin; (ii) 16-doxyl-stearic acid bound to a second, low-affinity fatty-acid binding site on albumin; (iii) ''free'' 16-doxyl-stearic acid in serum; (iv) a very minor component (about 500 times less than the others) of 16-doxyl-stearic acid aggregates. It was found that the diagnostic sensitivity and specificity of the test were 87.4% and 95.7%, respectively for differentiating healthy individuals from cancer patients, and 87.4% and 85.7% for differentiating cancer patients from chronic disease patients. Thus the results are impressive. Furthermore, from a serial evaluation of changes in albumin conformation, followed during the progression of their disease, an excellent accord was found between the extent of abnormality according to the ESR results and those from clinical and pathological examination of the severity of the disease. It is concluded therefore, that ESR may provide a non-invasive diagnostic method for cancer patients, and which may furthermore provide a means to monitor the course of the disease once its presence is established.

13. Detection of hydrogen peroxide by ESR in tissue[137]

Using a spin-trapping technique, the spin-trap, 1-hydroxy-3,3,5,5-tetramethyl-3-imidazoline-3-oxide was used to detect hydrogen peroxide (as decomposed to $^{\bullet}OH$ radicals) in porcine coronary microvessels and epicardial arteries. The tissue was incubated in Krebs' solution containing indomethicin and aminotriazole with or without tiron or PEG-SOD, which was bubbled with 95% O_2 and 5% CO_2. After 30 minutes incubation and centrifugation, the filtrates were added to the spin-trap, p-acetamidophenol and horseradish peroxidase and further incubated for 60 seconds at 37°C. The H_2O_2 was decomposed to $^{\bullet}OH$ radicals which gave rise to a characteristic ESR spectrum from the stable spin-adduct with the spin-trap. The relative signal intensity was determined against an Mn^{2+} marker as a standard. The H_2O_2 concentration was gauged from the relative ESR signal-intensity *vs* H_2O_2 concentration deduced as a preliminary calibration.

14. ESR Measurement of the intracellular water volume in human sperm[138]

In relation to fertility, studies of the sperm volume in animals, bull, ram, rabbit, rooster, boar, stallion, and also that of human sperm have been made using ESR and various spin-probes. Tempone dissolves in and hence reveals an ESR signal from all aqueous regions, intracellular, and extracellular, and the membrane-impermeable line-broadening agent potassium chromium oxalate is used to broaden the extracellular signal almost to the point of rendering it invisible. To further minimize the extracellular signal, background control spectra were digitally subtracted from the sample spectra to eliminate background interference. It is important to stress that this approach measures only the water volume of sperm cells and not the total aqueous volume, including dissolved salts and proteins. From calibration spectra of ESR signal intensity *vs* volume at a given concentration of Tempone in water, the intracellular water volume may be deduced. The parameter of interest is the total cell volume, which may be obtained from the percentage of cell water volume to the total volume, as obtained from the relative wet-to-dry mass ratios. Assuming that the cell water volume of sperm is 59% of the total, cell volumes of 34 and 42 μm^3 were derived from two experimental series.

15. Studies on enzymes

Studies of enzyme active-site ''units'' remain an active province of ESR in the biological fields. A good example is a paper which describes spectroscopic and electronic structure determinations of the class I Escherichia coli ribonucleotide reductase (RNR) intermediate X along with computational results for three model complexes that are considered in orded to determine the electronic structure and and geometry of the Fe-III/Fe-IV active site of the intermediate X. The intermediate X was trapped by rapid freeze-quenching (RFQ) and characterised using a combination of EPR, absorption, and MCD, for the species in R2 wild-type (WT) and two variants, W48A and Y122F/Y356F. The relative contributions of intermediate X and radicals present were established by spin-counting, while RFQ-MCD was used specifically to probe the nature of the Fe-III/Fe-IV active site, which displayed three Fe^{IV} d–d transitions between 16,700 and 22,600 cm^{-1}, two Fe^{IV} d–d spin-flip transitions between 23,500 and 24,300 cm^{-1}, and five oxo to Fe^{IV} and Fe^{III} charge transfer (CT) transitions between 25,000 and 32,000 cm^{-1}. Since the Fe^{IV} d–d transitions were perturbed in the two variants, it was confirmed that all three d–d transitions derive from the d-π manifold. Significantly, the large Fe^{IV} d–π splittings in the WT are incompatible with a bis-μ-oxo structure. It is concluded that the Fe^{IV} d–d transitions in WT intermediate X are best ascribed to a bridged μ-oxo/μ-hydroxo $[Fe^{III}(\mu-O)(\mu-OH)Fe^{IV}]$ structure. The authors stress that the μ-oxo/μ-hydroxo core structure provides an important $\sigma-\pi$ super-exchange pathway, which is not present in the bis-μ-oxo structure, and can promote facile electron transfer from Y122 to the remote Fe^{IV} unit *via* the bent oxo bridge, thereby generating the catalytically important tyrosyl radical[139]. A review discusses recent experimental advances that have significantly increased the potential of EPR and electron nuclear double resonance (ENDOR) methods to characterize the structure and dynamics of metalloproteins, which include the introduction of powerful pulsed EPR/ENDOR methods and the development of spectrometers operating at very high microwave frequencies and high magnetic fields. Applications to iron-, nickel-, cobalt- and copper-containing proteins are particularly highlighted[140]. A determination of the catalytically active tyrosyl radical in ovine prostaglandin H_2 synthase-1 has been undertaken using high-frequency pulsed EPR and ENDOR methods. The radical is signified by the so called ''wide doublet'' signal, but further structural elucidation was rendered possible in the 130 GHz

ENDOR spectra which revealed a hydrogen-bonded deuteron in partially deuterium oxide exchanged samples. In order to obtain a satisfactory simulation of the ENDOR spectra, it was found necessary to incorporate a distribution of H-bond distances, and which was consistent with the model employed to account for the distribution in g_x values detected in pulsed high-field EPR spectra from these samples[141]. In a study of Rhodothermus marinus (a thermohalophilic Gram negative bacterium which contains a type I NADH/quinone oxidoreductase–''complex 1'') it was demonstrated that the stoichiometry of NADH oxidation and quinone reduction is 1 : 1. By improving the isolation procedure, sufficiently large amounts of protein were obtained that the material could be thoroughly characterized by EPR spectroscopy, employing a range of temperatures and microwave powers, and in using NADH, NADPH, and dithionite as reducing agents. A minimum of two $[2Fe-2S]^{2+/1+}$ and four $[4Fe-4S]^{2+/1+}$ centres were determined in the purified complex, while ESR-detected redox-titrations permitted the measurement of the reduction potentials of the iron-sulfur centres. Apart from one of the $[4Fe-4S]^{2+/1+}$ centres, which has a lower reduction potential, the other centres were found all to have reduction potentials of -240 ± 20 mV, at pH 7.5[142]. The outer mitochondrial membrane protein mitoNEET was discovered as a binding target of pioglitazone, an insulin-sensitizing drug of the thiazolidinedione class used to treat type 2 diabetes[143], and has been shown to be a member of a small family of proteins containing a 39-amino-acid CDGSH domain[144]. While the CDGSH domain is annotated as a zinc finger motif, mitoNEET was found also to contain iron, and on the basis of optical and EPR measurements the presence of a redox-active pH-labile Fe–S cluster was established. Spectroscopic studies of recombinant proteins showed that the 2Fe–2S cluster was coordinated by Cys-3 and His-1, and furthermore the His ligand was proved to be a feature in the observed pH lability of the cluster, indicating that the release of the cluster was triggered by loss of this ligand *via* protonation. mitoNEET is the first 2Fe–2S-containing protein located in the outer mitochondrial membrane to be identified, and it is speculated that mitoNEET may function in Fe–S cluster shuttling and/or in redox reactions[145]. NADH : quinone oxidoreductase (complex 1) is an essential protein in cellular energy production since it utilises a series of redox cofactors to couple electron transfer to the generation of a proton-motive force across the inner mitochondrial or bacterial cytoplasmic membrane. There is a noncovalently bound flavin mononucleotide at the active site of complex 1, which

enables NADH oxidation, along with eight or nine iron-sulfur clusters which together transfer electrons between the flavin and a quinone-binding site. In order to comprehend the mechanism of complex 1, the properties of these clusters must be determined, both individually and as a collective functional moeity. EPR spectra were recorded from the overexpressed NuoG subunit from Escherichia coli complex 1 and were compared with those from the intact enzyme, from which it is concluded that couplings from N4 and N5 have been misassigned in previous investigations: *i.e.* signal N4 is from Nuol (not NuoG) and signal N5 is from the conserved cysteine-ligated [4Fe−4S] cluster in NuoG (not from the cluster with a histidine ligand). The implications of these reassignments for the free energy profile for electron transfer through complex 1 are discussed[146]. While many ferritin structures from bacteria to mammals have been reported, until now only one was available from archaea, the ferritin from Archaeoglobus fulgidus (AfFtn). The PfFtn 24-mer exhibits the 432 point-group symmetry that is characteristic of most ferritins, a fact that indicates that the 23 symmetry reported previously for AfFtn is not a general characteristic of archaeal ferritins. The ferroxidase centre of the aerobically crystallized ferritin contains one iron at site A and at sites B and C only upon steeping in iron or zinc solutions. EPR measurements suggest that this depletion of iron from the native ferroxidase centre is a consequence of a iron-complexation by the crystallization salt. The extreme thermostability of PfFtn is compared with that of eight structurally similar ferritins and is proposed to originate mostly from the observed high number of intrasubunit hydrogen bonds[147].

Many properties of copper-containing nitrite reductase *e.g.* gene expression, enzyme activity, and substrate affinity are pH-dependent. One paper reports the use of a combination of techniques to investigate the structural basis for the pH dependence of activity and nitrite affinity by examining the type 2 copper site and its immediate surroundings in nitrite reductase from *Rhodobacter sphaeroides* 2.4.3. When co-crystallized with substrate, nitrite is shown to bind in a bidentate fashion with its two oxygen atoms ligating the type 2 copper, overlapping with the positions occupied by the solvent ligand in the high and low pH structures, according to X-ray diffraction measurements. The pH dependence of the binding of nitrite to the active site was determined using FT IR, and EPR spectroscopy to characterize the pH dependence of the reduction potential of the type 2 copper site[148]. DFT calculations were employed in a study of the spin-density distribution, g tensors, and Cu and ligand hyperfine tensors for blue copper proteins

plastocyanin and stellacyanin, and for small model complexes. It inferred that the bulk of the spin density is almost equally shared by the copper atom and the sulfur atom of the equatorial cysteine ligand. The influence of spin-orbit coupling on the EPR parameters may be appreciable, and especially spin-orbit effects on the ^{65}Cu hyperfine coupling tensors in blue copper sites are found to be unusually large compared to more regularly coordinated Cu^{II} complexes with similar spin density on copper[149].

16. Advanced ESR methods, applied to proteins, lipids and cyclodextrins

A review has appeared concerning he use of site-directed spin labelling in the characterisation of the structure of proteins. In particular, the use of pulsed techniques to establish long-range distances and distributions in proteins is considered, and methods to determine the conformations and local dynamics of spin-labelled side-chains, and how these may influence ESR lineshapes[150]. Another review deals with the simulation of very high field EPR spectra of spin-labelled lipids in membranes. It is emphasised that the lateral ordering of the lipid chains is characterised by the g_{xx}/g_{yy} tensor components, and which can be determined by the theory of motional narrowing, but the spin-Hamiltonian parameters must be correct to account for changes in the differential polarity that exists within the membrane environment. When the applied magnetic field is very high, the spectra are found to be sensitive only to local segmental motion of the lipid chains[151]. Solvent effects on magnetic parameters of nitroxide spin labels in combination with side-directed spin-labeling EPR methods provide very useful means for elucidating polarity profiles in lipid bilayers and mapping local electrostatic effects in complex biomolecular systems. One major contributor to these solvent effects is the hydrogen bonds that could be formed between the nitroxide moiety and water and/or the available hydroxyl groups. Here, formation of hydrogen bonds between a lipid bilayer spin probe 5-doxyl stearic acid, Scheme 4, 5DSA and hydrogen-bond donors has been studied using high-frequency (HF) pulsed ENDOR and EPR. A hydrogen-bonded deuteron was directly detected by ENDOR at a frequency of 130 GHz from 5 DSA dissolved in different deuterium substituted alcohols, while the characteristic signal was absent in the nonpolar medium, toluene-d_8. The geometry of the hydrogen bond and its length of 1.74 ± 0.06 Å, were found to be practically the same for all four alcoholic media,

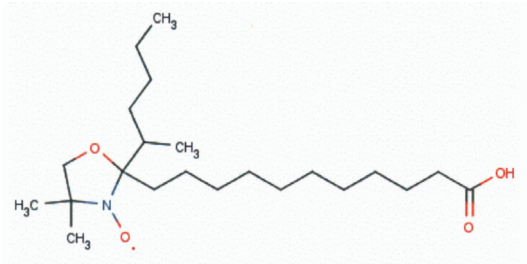

Scheme 4 *Molecular structure of 12-DOXYL stearic acid.*

indicating that nearly identical hydrogen bonds were formed irrespective of the solvent polarity. HF EPR spectra appear to be particularly sensitive to the investigation of hydrogen bonds and potentially the method could be used for probing the hydrogen-bond network in complex biomolecular assemblies and lipid bilayers that have been rendered paramagnetic using site-directed spin-labelling methods[152]. A report has appeared of a site-directed spin-labelling study of 10-mer RNA duplexes and HIV-1 TAR RNA motifs possessing a range of spin-spin distances. The labels were attached to the 2′-NH2 positions of given uridines in the duplexes, and their interspin distances were measured using molecular dynamics simulations (MD) and also Fourier deconvolution methods (FD). According to the MD results, the 10-mer duplexes were found to have interspin distances ranging from 10 to 30, whereas dipolar line broadening of the CW EPR spectrum is only observed for expected spin-spin separations in the range 10–21 Å but is absent for distances greater than 25 Å. The conformational changes in TAR (transactivating responsive region) RNA in the presence and in the absence of different divalent metal ions were monitored by measuring distances between two nucleotides in the bulge region. These results demonstrate that EPR spectroscopy provides potentially powerful ‘‘ruler’’ as an aid to the prediction of the structures of RNA molecules[153]. A study has been made of the hydration behaviour of dimyristoyl-phosphatidylglycerol (DMPG) and dimyristoyl-phosphatidylcholine (DMPC) vesicles as a functions of both salt concentration and temperatures above the lipid phase transition. In order to achieve motionally narrowed ESR spectra, the small spin probe di-*tert*-butyl nitroxide (DTBN) was used. The novelty of the approach presented rests upon the recording of the second harmonic ESR signal which is then analysed by a line-fitting procedure. Spectral fitting yields precise FSR parameters and provides a precise view of the local environment of the spin probe in both lipid and aqueous phases. The ^{14}N hyperfine coupling constant arising from DTBN that occupies the vesicles yields a measure of the hydration state of the negatively

charged vesicle surface, which is affected by the addition of salt, while the hydration of DMPC vesicles is not influenced by salt concentration at the low temperatures. In contrast, the salt concentration does affect the degree of hydration at higher temperatures, as is thought due to the faster motion of the phospholipid molecules. The spin probe exhibits anisotropic motion in the phospholipid bilayer, the extent of which is greater as the salt concentration increases[154]. A review has been published on the subject of determining 1.5–10 nanometre distances using pulsed ESR[155]. Results from pulsed electron double resonance (ELDOR) measurements have been reported to determine the distances between the spin-centres in a FAD-dependent sulfydryl oxidase, Augmenter of Liver Regeneration (ALR). ALR is a homodimer in which each subunit contains a noncovalently bonded FAD cofactor. Both FAD units may be converted into their blue neutral radical forms, and using three and four pulse sequence experiments, a distance of 26.1 ± 0.8 Å was obtained[156]. An ESR study of guest–host complexes of beta- and gamma-cyclodextrins (CDs) with two spin-labelled indole derivatives in aqueous solutions along with theoretical calculations of these systems is reported. It is found that the presence of CD causes a reduction in the polarity of the NO group environment, while the rotational correlation time of guest molecules increases. The indole derivatives have different structures but identical molecular weights and both form I : I complexes with gamma-CD. On the basis of ESR spectral simulation, it was possible to determine the orientation of the indole ring in relation to the plane of the host molecule and the rotational diffusion coefficients of the complexes, which corresponded to the hydrodynamic volume of one gamma-CD molecule. In contrast to the complexes with gamma-CD the rotational correlation times, T, of the complexes with beta-CD correspond to a hydrodynamic volume which much exceeds the volume of a single beta-CD molecule[157]. The synthesis is reported of two isomers of permethylated beta-cyclodextrin, labelled with paramagnetic TEMPO moieties attached on the same rim of the cavity, whose host-guest properties were subsequently investigated by EPR spectroscopy[158]. It is known that the EPR spectra of cyclodextrins (CD) labelled with TEMPO are sensitive to the incorporation of large guest molecules. In a study of spin-labelled CD's in concentrated poly(ethylene glycol)/poly(propylene glycol) solutions, marked departure was noted from the Debye–Stokes–Einstein rotational diffusion model, which is suggested due to self-aggregation of alkylene glycols given their high concentration. The work was extended to an investigation of adamantane-functionalised DAB dendrimers, for which it was found that the binding-strength increased with the order of dendrimer generation (size), and that

supramolecular aggregates are formed in high concentrations with the generation 3 dendrimer[159]. Using cw-EPR and pulsed EPR, interactions of spin-labelled polyamidoamine dendrimers, termed G_n, where n indicates the generation (number of amidoamine layers), at different protonation levels with selected amino acids and proteins were investigated. Gly, Glu, Arg, and Leu were selected as being representative of neutral (zwitterionic)-polar, acidic, basic, and low-polar amino acids, respectively, while the water-soluble proteins alpha-chymotrypsin and albumin were selected on the basis of a basic and an acidic isoelectric point, respectively. Typically, dendrimers at a high protonation level interact stronger with amino acids than do those at a low level of protonation, but even for highly protonated dendrimers, a synergistic effect between hydrophilic and hydrophobic interactions was noted to promote the formation of stable G_n-amino acid adducts, as demonstrated by the enhanced interactions with Leu. As expected from acid–base interactions, stable adducts were formed between Arg and highly protonated dendrimers and between Glu and low level protonated dendrimers. Simulation of the ESE traces gave results that are consistent with the cw-EPR results from which it is concluded that a partial complexation of the nitroxides of the dendrimer with Leu and alpha-chymotrypsin occurs[160]. The novel peptide-bound nitronylnitroxides [1-(1′,3′-dioxyl-4′,4′,5′,5′-tetramethyldihydroimidazol-2-yl)-phenyl-4-yl]oxyacetic acid (1), and its peptide derivatives (2) (X_{aa} = Ala, Gly, Gln), were synthesized and their ESR spectra recorded. The activity of (2) toward scavenging free radicals was assessed *in vitro* and the throbolysis effect of the material was determined by means of an euglobulin clot test, a fibrinolytic lysis test and *in vivo* thrombolysis tests. It was concluded that (2) is active both as a free radical scavenger and a thrombolytic agent[161].

References

1. Carrington, A. and McLachlan A. (1967). *Introduction to magnetic resonance*. London: Harper and Row. ISBN 0470265728.
2. http://en.wikipedia.org/wiki/Electron_paramagnetic_resonance#cite_note-lowd-6
3. Swartz, H.M. *et al*. (2004) *NMR Biomed*., **17**, 335.
4. Swartz, H.M. *et al*. (2007) *Radiat. Meas*., **42**, 1075.
5. Dunne, J. *et al*. (2006). *Biochem. J*., **399**, 513.
6. Fujita, Y. *et al*. (2005) *Forensic Science International*, **152**, 39.

7. Fossey, J., Lefort, D. and Sorba, J. (1995) *Free radicals in organic chemistry.* Wiley, Chichester.
8. Wertz, J.E. and Bolton, J.R. (1972) *Electron spin resonance: theory and practical applications*. McGraw-Hill, New York.
9. Rhodes, C.J. (ed.) (2000) *Toxicology of the human environment - the critical role of free radicals*. Taylor and Francis, London.
10. Perkins, M.J. (1980) *Adv. Phys. Org. Chem*., **17**, 1.
11. Swartz, H.M. and Timmins, G.S. (2000) In: Rhodes, C.J. (ed.), *Toxicology of the human environment - the critical role of free radicals*, p. 91. Taylor and Francis, London.
12. Mitchell, J.B. *et al*. (2000) In: Rhodes, C.J. (ed.), *Toxicology of the human environment - the critical role of free radicals*, p. 113. Taylor and Francis, London.
13. Tomasi, A. and Iannone, A. (1993) In: *Biological Magnetic Resonance*, Berliner, L.J. and Reuben, J. (eds.), Vol. 13, Plenum Press, New York, p 353.
14. Ichimori, K. *et al*. (1993) *Free Rad. Res. Comms*., S129.
15. Towner, R.A. (2000) In: Rhodes, C.J. (ed.), *Toxicology of the human environment - the critical role of free radicals*, p. 8. Taylor and Francis, London.
16. Janzen, E.G. *et al*. (1985) *Environ. Health Perspects*., **64**, 151.
17. Eberson, L. (2000) In: Rhodes, C.J. (ed.), *Toxicology of the human environment - the critical role of free radicals*, p. 25. Taylor and Francis, London.
18. Buettner, G.R. and Sharma, M.K. (1993) *Free Rad. Res. Commun*., **19**, S227.
19. Iwahashi, H. *et al*. (1991) *Arch. Biochem. Biophys*., **285**, 172.
20. Hiraoka, W., Kuwabara, M. and Sato, F. (1991) *Int. J. Radiat. Biol*., **59**, 875.
21. Mason, R.P. (2000) In: Rhodes, C.J. (ed.), *Toxicology of the human environment - the critical role of free radicals*, p. 50. Taylor and Francis, London.
22. Lai, E.K. *et al*. (1979) *Biochem. Pharmacol*., **28**, 2231.
23. Tomasi, A. *et al*. (2000) In: Rhodes, C.J. (ed.), *Toxicology of the human environment - the critical role of free radicals*, p. 71. Taylor and Francis, London.
24. Janzen, E.G. (1987) *Free Rad. Res. Commun*., **3**, 357.
25. Knecht, K.T., DeGray, J.A. and Mason, R.P. (1992) *Mol. Pharmacol*., **41**, 943.
26. Di Luzio, N.R. (1963) *Physiologist*, **6**, 169.
27. Slater, T.F. (1972) *Free radical mechanisms in tissue injury*, Pion Ltd., London.
28. Knecht, K.T., Bradford, B.U. and Mason, R.P. (1990) *Mol. Pharmacol*., **38**, 26.
29. Tran, T.T. *et al*. (2000) *Pest. Manag. Sci*., **56**, 818.
30. Rhodes, C.J., Tran, T.T. and Morris, H. (2004) *Spectrochim. Acta A*, **60**, 1401.
31. Roselaar, S.E. *et al*. (1995) *Kidney Int*., **48**, 199.
32. Singh, D. *et al*. (1995) *Ann. Rheum. Dis*., **54**, 94.
33. Nazhat, N.B. *et al*. (1990) *Biochem. Biophys. Res. Commun.*, **166**, 807.
34. Stolze, K. and Mason, R.P. (1987) *Biochem. Biophys. Res. Commun*., **143**, 941.
35. Ozawa, T. and Hanaki, H. (1987) *Biochem. Biophys. Res. Commun*., **142**, 410.
36. Ozawa, T. and Hanaki, A. (1986) *Biochem. Biophys. Res. Commun*., **136**, 657.

37. Kohno, M. *et al*. (1991) *Bull. Chem. Soc. Jpn*., **64**, 1447.
38. Ozawa, T. and Hanaki, A. (1991) *Bull. Chem. Soc. Jpn*., **64**, 1976.
39. Guo, R. *et al*. (2002) *Biochem. Biophys. Acta*, **1572**, 133.
40. Chandra, H., Keeble, D.J. and Symons, M.C.R. (1988) *J. Chem. Soc., Faraday Trans., 1*, **84**, 609.
41. Davies, C.A. *et al*. (2001) *Nitric oxide: Biology and Chemistry*, **5**, No. 2, 116.
42. Nazhat, N.B. (1999) *Biochim. Biophys. Acta*, **1427**, 276.
43. Mulsch, A., Mordvintcev, P. and Vanin, A. (1992) *Neuroprotocols: A Companion to Methods in Neurosciences*, **192**, Vol. 1, No. 2, 165.
44. Grootveld, M. and Rhodes, C.J. (1995) In: Blake, D. and Winyard, P.G. (eds.), *Immunopharmacology of free radical species*. p. 3. Academic Press, San Diago.
45. Clement, B. *et al*. (1994) *Arch. Pharm. (Weinheim)*, **327**, 793.
46. Olesen, S.P. *et al*. (1997) *Acta Neurol. Scand*., **95**, 219.
47. Mordvintcev, P. *et al*. (1991) *Analyt. Biochem*., **199**, 142.
48. Arroyo, C.M. and Kohno, M. (1991) *Free Rad. Res. Commun*., **14**, 145.
49. Park, J.S.B. and Walton, J.C. (1997) *J. Chem. Soc., Perkin Trans*., **2**, 2579.
50. Gabr, I. and Symons, M.C.R. (1996) *J. Chem. Soc., Faraday Trans*., **92**, 1769.
51. Korth, H.-G. *et al*. (1992) *Angew. Chem. Int. Ed. Engl*., **31**, 891.
52. Yordanov, N.D., Novakova, E. and Lubenova, S. (2001) *Anal. Chim. Acta*, **437**, 131.
53. Halliwell, B. and Gutteridge, J.M.G. (1989) *Free radicals in biology and medicine*. Clarendon Press, Oxford.
54. Swartz, H.M. *et al*. (1994) *Adv. Exp. Med. Biol*., **361**, 119.
55. James, P.E. *et al*. (1997) *Magn. Reson. Med*., **38**, 48.
56. Boyer, S.J. and Clarkson R.B. (1994) *Colloids Surf*., **82**, 217.
57. Atsarkin, V.A. *et al*. (2001) *J. Mag. Reson*., **149**, 1.
58. Jordan, B.F., Baudelet, C. and Gallez, B. (1998) *Magn. Reson. Mater. Phys. Biol. Med*., **7**, 121.
59. Liu, K.J. *et al*. (1994) *Biophys. J*., **67**, 896.
60. Regulla, D. (2000) *Appl. Radiat. Isot*., **52**, 1023.
61. Ikeya, M. *et al*. (2000) *Appl. Radiat. Isot*., **52**, 1209.
62. Lund, A. *et al*. (2002) *Spectrochim. Acta A*, **58**, 1301.
63. Joint FAO/AEA/WHO Expert Committee, *Wholesomeness of irradiated food*, 1981, WHO, Geneva, No. 659.
64. Piccerelle, P. *et al*. (2000) *J. Pharma. Belg*., **55**, 131.
65. Ambroz, H. *et al*. (2000) *Radiat. Phys. Chem*., **58**, 357.
66. Raffi, J. *et al*. (2002) *Spectrochim. Acta A*, **58**, 1313.
67. Raffi, J. and Belliardo, J.-J. (1991) *Potential new methods in identification of irradiated food*, CE, Luxembourg, EUR 13331 EN.
68. Douifi, L. *et al*. (1998) *Spectrochim. Acta A*, **54**, 2403.
69. Raffi, J. (1998) *Trends. Anal. Chem*., **17**, 226.
70. Raffi, J. and Stocker, P. (1996) *Appl. Magn. Reson*., **10**, 357.

71. Dodd, N., Swallow, A.J. and Ley, F. (1985) *Radiat. Phys. Chem*., **26**, 451.
72. Desrosiers, M. (1996) *J. Appl. Radiat. Isot*., **47**, 1621.
73. Rafi, J.J. *et al*. (1988) *J. Chem. Soc., Faraday Trans. 1*, **84**, 3359.
74. Kocherginsky, N. and Swartz, H.M. (1995) *Nitroxide spin labels*. CRC Press, Boca Raton.
75. Swartz, H.M. and Walczak, T. (1996) *Res. Chem. Intermed*., **22**, 511.
76. Belkin, S. *et al*. (1987) *Arch. Biochem. Biophys*., **256**, 232.
77. Morris, G. *et al*. (1991) *J. Pharm. Sci*., **80**, 149.
78. Schara, M., Pecar, S. and Svetek, J. (1990) *Colloids Surf*., **45**, 303.
79. Marsh, D. (1981) In: Grell, E. (ed.), *Membrane spectroscopy*, p. 15. Springer Verlag, Berlin.
80. Seelig, J. (1976) In: Berliner, L.J. (ed.), *Spin labelling: theory and applications*, p. 373. Academic Press, New York.
81. Chen, K., Morse II, P.D. and Swartz, H.M. (1983) *Biochem. Biophys. Acta*, **943**, 477.
82. Sentjurc, M., Morse II, P.D. and Swartz, H.M. (1986) *Period. Biol*., **88**, 202.
83. Bartosz, B. and Gwodzinski, K. (1983) *Am. J. Hematol*., **14**, 377.
84. Gwodzinski, K., Bartosz, B. and Leyko, W. (1982) *Stud. Biophys*., **89**, 141.
85. Gwodzinski, K. (1986) *Radiat. Environ. Biophys*., **25**, 107.
86. Gwodzinski, K. (1985) *Stud. Biophys*., **106**, 43.
87. Chen, K. and McLaughlin, M.G. (1985) *Biochem. Biophys. Acta*, **845**, 189.
88. Gascoyne, P., Pethig, R. and Szent-Gyorgi, A. (1987) *Biochem. Biophys. Acta*, **923**, 257.
89. Nahl, S. *et al*. (1988) *Physiol. Chem. Phys. Med*., **20**, 183.
90. Kieber, D.J., Johnson, C.G. and Blough, N.V. (1992) *Free Rad. Res. Commun*., **16**, 35.
91. Chen, K. and Swartz, H.M. (1989) *Biochem. Biophys. Acta*, **992**, 131.
92. Hockel, M.K. (1996) *Cancer Res*., **6**, 4509.
93. Hockel, M.K. (1996) *Sem. Radiat. Oncol*., **6**, 3.
94. Vaupel, P. (1996) *Experimentia*, **52**, 464.
95. Gabrijelcic, V. and Sentjurc, M. (1995) *Int. J. Pharm*., **118**, 207.
96. Gabrijelcic, V., Sentjurc, M. and Kristl, J. (1990) *Int. J. Pharm*., **62**, 75.
97. Gabrijelcic, V., Sentjurc, M. and Schara, M. (1991) *Period. Biol*., **93**, 245.
98. Gabrijelcic, V., Sentjurc, M. and Schara, M. (1994) *Int. J. Pharm*., **102**, 151.
99. Fuchs, J. *et al*. (1997) *Free Rad. Biol. Med*., **22**, 967.
100. http://www.cyberlipid.org/perox/oxid0002.htm
101. Burton, G.W., Foster, D.O., Perley. B., Slater, T.F., Smith. I.C.P. and Ingold, K.U. (1985) *Philos. Trans. R. Soc. Lond. B*, **311**, 565–578.
102. Gutteridge, J.M.C. (1978) *Res. Commun. Chem. Pathol. Pharmacol*., **22**, 563–571.
103. Zhu, J. *et al*. (1990) *J. Phys. Chem.*, **94**, 7185.
104. Sevilla, C.L., Becker, D. and Sevilla, M.D. (1986) *J. Phys. Chem*., **90**, 2963–2968.

105. Yanez, J., Sevilla, C.L., Becker, D. and Sevilla, M.D. (1987) *J. Phys. Chem*., **91**, 487.
106. Zhu, J. and Sevilla, M.D. (1990) *J. Phys. Chem*., **94**, 1447.
107. Muller, S.N., Batra, R., Senn, M., Geise, B., Kisel. M. and Shadyro, O. (1997) *J. Am. Chem. Soc*., **119**, 2795.
108. Shi, X.L., Rojanasakul, Y., Gannet, P., Liu, K.J., Mao, Y., Daniel, L.N., Ahmed, N. and Saffiotti, U. (1994) *J. Inorg. Biochem*., **56**, 77.
109. Rhodes, C.J., Hinds, C.S. and Reid, I.D. (1997) *Free Rad. Res*., **27**, 347–352.
110. Karoui, H., Hogg, N., Frejaville, C., Tordo, P. and Kalyanaraman, B. (1996) *J. Biol. Chem*., **271**, 6000.
111. Karoui, H., Hogg, N., Joseph, J. and Kalyanaraman, B. (1996) *Arch. Biochem. Biophys*., **330**, 115.
112. Jiang, J.J., Liu, K.J., Jordan, S.J., Swartz, H.M. and Mason, R.P. (1996) *Arch. Biochem. Biophys*., **330**, 266.
113. Stoyanovsky, D.A. and Cederbaum, A.I. (1996) *Biochemistry*, **35**, 15839.
114. Tezuka, M., Ishii, S. and Okada, S. (1991) *J. Inorg. Biochem*., **44**, 261–265.
115. Hanna, P.M., Kadiiska, M.B., Jordan, S.J. and Mason, R.P. (1993) *Chem. Res. Toxicol*., **6**, 711.
116. Rikans, L.E., Hornbrook, K.R. and Cai, Y. (1994) *Mech. Age. Devel*., **76**, 89.
117. Shi, X.L., Dong, Z.G., Dalal, N.S. and Gannett, P.M. (1994) *Biochim. Biophys. Acta–Molec. Basis Dis*., **1**, 65.
118. Kikugawa, K., Hiramoto, K., Okamoto, Y. and Hasegawa, Y.K. (1994) *Free Rad. Res*., **21**, 399.
119. Hempenius, R.A., Rietjens, I.M.C.M., Grooten, H.N.A. and Devries, J. (1992) *Toxicology*, **73**, 23–34.
120. Kramer, J.H., Dickens, B.F., Misic, V. and Weglicki, W.B. (1995) *J. Molec. Cell. Cardiol*., **27**, 371.
121. Barr, D.P. and Mason, R.P. (1995) *J. Biol. Chem*., **270**, 12709.
122. Barr, D.P., Martin, M.V., Guengerich, F.P. and Mason, R.P. (1996) *Chem. Res. Toxicol*., **9**, 318.
123. Rota, C., Barr, D.P., Martin, M.V., Guengerich, F.P., Tomasi, A. and Mason, R.P. (1997) *Biochem. J*., **328**, 565.
124. Berliner, L.J. (ed.) (1976) *Spin-labelling: theory and applications*. Academic Press, New York.
125. Knowles, P.F. and Marsh, D. (1991) *Biochem. J*., **274**, 625.
126. Marsh, D. and Horvath, L.I. (1989) In: Hoff, A.J. (ed.), *Advanced ESR, applications in biology and biochemistry*. p. 707. Elsevier, Amsterdam.
127. Van Bilsen, D.G.J.L. and Hoekstra, F.A. (1993) *Plant Physiol*., **101**, 675.
128. Cassol, R., Ge, M.T., Ferriani, A. and Freed, J.H. (1997) *J. Phys. Chem*., **101**, 8782.
129. Patyal, B.R., Crepeau, R.H. and Freed, J.H. (1997) *Biophys. J*., **73**, 2201.
130. Xu, D.J., Crepeau, R.H., Ober, C.K. and Freed, J.H. (1996) *J. Phys. Chem.*, **100**, 15873.
131. Marsh, D. (1997) *Eur. Phys. J. Biophys. Lett*., **26**, 203.

132. Swamy, M.J. and Marsh, D. (1997) *Biochemistry*, **36**, 7403.
133. Marsh, D. (1996) *Braz. J. Med. Biol. Res*., **29**, 863.
134. Smirnov, A.I., Smirnova, T.I. and Morse, P.D. (1995) *Biophys. J*., **68**, 2350.
135. Janzen, E.G. (1974) Electron spin resonance. *Analyt. Chem*., **46**(5), 478 R.
136. Kazmierczak, S.C. *et al*. (2006) *Clin. Chem*., **52**(11), 2129.
137. Matoba, T. *et al*. (2003) *Arterioscler. Thromb. Vasc. Biol*., **23**, 1224.
138. Kleinhans, V.S. *et al*. (1992) *J. Androl*., **13**, 498.
139. Mitic, N. *et al*. (2007) *J. Am. Chem. Soc*., **129**, 9049.
140. Van Doorslaer, S. and Vinck, E. (2007) *Phys. Chem. Chem. Phys*., **9**, 4620.
141. Wilson, J.D., Wu, G., Tsai, A.-L. and Gerfen, G.J. (2005) *J. Am. Chem. Soc*., **127**, 1618.
142. Fernandes, A.S., Sousa, F.L., Teixeira, M. and Pereira, M.M. (2006) *Biochemistry*, **45**, 1002.
143. Colca, J.R. (2004) *Am. J. Physiol*., **286**, E252.
144. Wiley, S.E. *et al*. (2007) *Proc. Natl. Acad. Sci. USA*, **104**, 5318.
145. Wiley, S.E. (2007) *J. Biol. Chem.*, **282**, 23745.
146. Yukovlev, G., Reda, T. and Hirst, J. (2007) *Proc. Natl. Acad. Sci. USA*, **104**, 12720.
147. Tatur, J., Hagen, W.R. and Matias, P.M. (2007) *J. Biol. Chem*., **12**, 615.
148. Jacobson, F. *et al*. (2007) *J. Biol. Chem*., **282**, 6347.
149. Remenyi, C., Reviakine, R. and Kaupp, M. (2007) *J. Phys. Chem. B*, **111**, 8290.
150. Fanucci, G.E. and Cafiso, D.S. (2006) *Curr. Opin. Struct. Biol*., **16**, 644.
151. Livshits, V.A. and Marsh, D. (2004) *Biol. Magn. Reson*., **22**, 431.
152. Smirnova, T.I., Smirnov, A.I., Paschenko, S.V. and Poluektov, O.G. (2007) *J. Am. Chem. Soc*., **129**, 3476.
153. Kim, N.-K., Murali, A. and DeRose, V.J. (2004) *Chem. Biol*., **11**, 939.
154. Peric, M., Alves, M. and Bales, B.L. (2004) *Biochim. Biophys. Acta*, **1669**, 116.
155. Dzuba, S.A. (2005) *Russ. Chem. Rev.*, **74**, 619.
156. Kay, C.W.M. *et al*. (2006) *J. Am. Chem. Soc*., **128**, 76.
157. Livshits, V.A. *et al*. (2005) *Russ. Chem. Bull*., **54**, 1169.
158. Chechik, V. (2007) *New J. Chem*., **31**, 1726.
159. Chechik, V. and Ionita, G. (2006) *Org. Biomolec. Chem*., **4**, 3505.
160. Ottaviani, M.F. *et al*. (2004) *Langmuir*, **20**, 10238.
161. Zhan, M. *et al*. (2005) *J. Med. Chem*., **48**, 4285.